Precise Conformational Control Yielding Highly Potent and Exceptionally Selective BRD4 Degraders with Strong Antitumor Activity

Jiantao Hu,[#] Biao Hu,[#] Fuming Xu, Mi Wang, Chong Qin, Donna McEachern, Jeanne Stuckey, and Shaomeng Wang*

Read Online

ACCESS | Metrics & More | Article Recommendations | Supporting Information

BD-9136

BD-9136 (MV4;11 cell, 4 h)
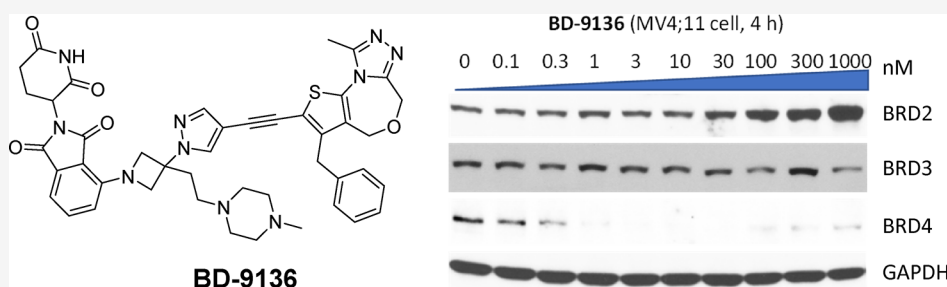
ABSTRACT: Starting from a nonselective bromodomain and extraterminal (BET) inhibitor and a cereblon ligand, we have used precise conformational control for the development of two potent and highly selective BRD4 degraders, BD-7148 and BD-9136. These compounds induce rapid degradation of BRD4 protein in cells at concentrations as low as 1 nM and demonstrate ≥1000-fold degradation selectivity over BRD2 or BRD3 protein. Proteomic analysis of >5700 proteins confirmed their highly selective BRD4 degradation. A single dose of BD-9136 selectively and effectively depletes BRD4 protein in tumor tissues for >48 h. BD-9136 effectively inhibits tumor growth without adverse effects on mice and is more efficacious than the corresponding pan BET inhibitor. This study suggests selective degradation of BRD4 as a strategy for the treatment of human cancers and demonstrates a strategy for the design of highly selective PROTAC degraders.

INTRODUCTION

The bromodomain and extraterminal (BET) domain proteins, namely, BRD2, BRD3, BRD4, and testis-specific BRDT, function as histone readers and are powerful transcriptional coregulators.[1−4] BET proteins have been studied for over a decade as therapeutic targets for human cancers and other human diseases.[1−4] Each of these BET proteins contains two highly homologous bromodomains (BD1 and BD2), which are druggable sites for small-molecule inhibitors.[1−4] A large number of BET inhibitors have been reported since 2010[3−5] and 12 of them have progressed into clinical trials.[5−7] Notwithstanding the early enthusiasm concerning BET inhibitors as a new class of breakthrough cancer therapeutics, they failed to demonstrate robust clinical activity in leukemia and solid tumors[5−7] with the exception of the treatment of myelofibrosis.[8]

Because BET proteins are highly homologous proteins, first-generation BET inhibitors were found to target both domains of all BET protein members with similar potencies. It has become increasingly clear that while BET proteins share some overlapping functions, it is clear that each BET protein has its specific role in gene regulation, biological processes, and human diseases.[5,9,10] In addition, BD1 and BD2 in each BET member also have their specific roles in biological processes and human diseases[5,9,10] Therefore, it is highly desirable to develop domain selective inhibitors, as well as selective inhibitors to target individual BET members.

In the last few years, selective BD1 or BD2 inhibitors were discovered[9−12] and have enabled elucidation of the differential roles played by these two domains in gene transcription and human diseases. In addition, BRD4 inhibitors with >10-fold binding selectivity over BRD2 and BRD3 have been reported.[13,14]

In addition to the development of bromodomain inhibitors, the major advancement in induced target protein degradation using the PROTAC technology[15−19] has enabled the discovery of highly potent degraders of the BET proteins.[16,20−28] While most of the reported BET degraders induce degradation of
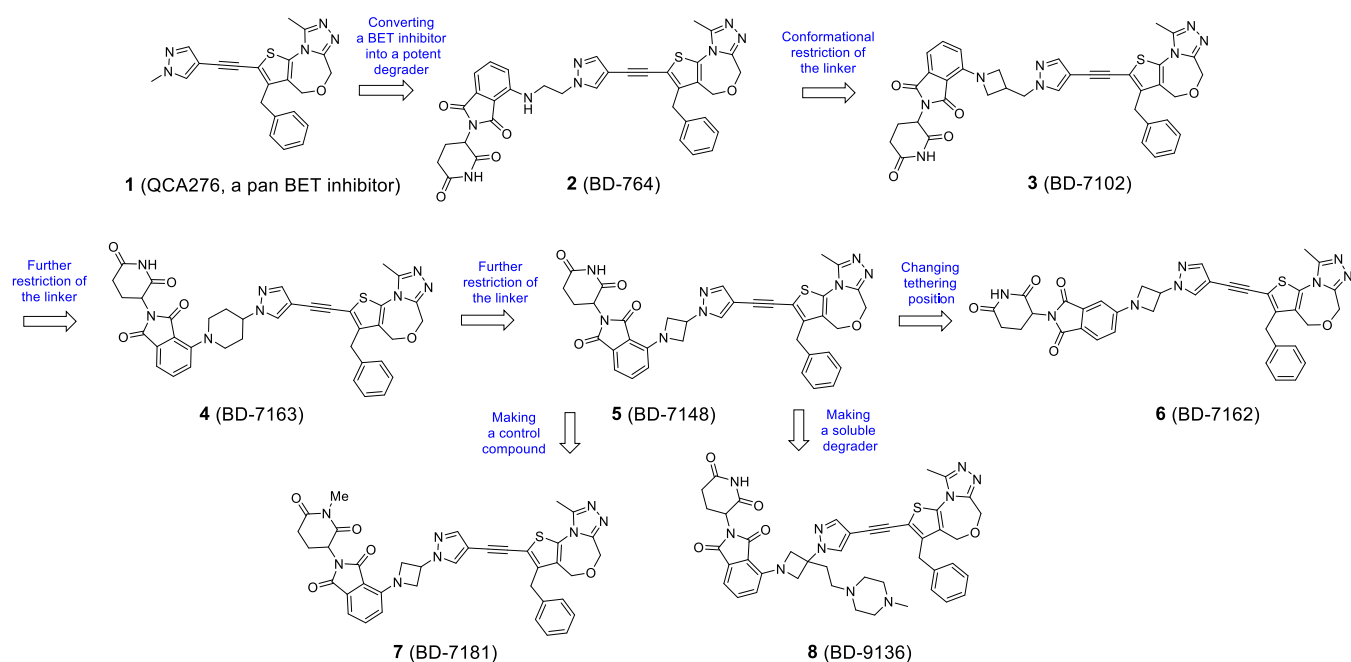
Figure 1. Design of BRD4 selective degraders through precise conformational control.

BRD2, BRD3, and BRD4 with similar potencies, compounds displaying selective degradation of BRD4 over BRD2 and BRD3 have been reported.[14,20,27] MZ1, reported by Ciulli et al.,[20] was the first selective BRD4 degrader and was designed using JQ1, a pan BET inhibitor, and a VHL-1 ligand. A subsequent study showed that MZ1 induced *de novo* contacts between BRD4 protein and VHL-1, forming a stable ternary complex and causing the selective degradation of BRD4 over that of BRD2 or BRD3.[24] ZXH-3-26 was discovered as another selective BRD4 degrader whose design was based upon JQ1 and a cereblon ligand.[27] ZXH-3-26 was shown to engage in unique interactions with BRD4 to achieve selective degradation of BRD4 over that of BRD2 or BRD3.[27] dBRD4-BD1 was recently reported as another BRD4 selective degrader.[14] In addition to these BRD4 selective PROTAC degraders, "molecular glue" degraders that demonstrate selectivity for BRD4/2 over BRD3 have been reported.[29,30]

In this study, we report the discovery of two highly potent and exceptionally selective BRD4 degraders BD-7148 and BD-9136. These two compounds achieve low-nanomolar degradation potencies against BRD4 and demonstrate >1000-fold degradation selectivity for BRD4 over BRD2 and BRD3 proteins. BD-9136 effectively and selectively depletes the levels of BRD4 protein in tumor tissues in mice with no significant effect on BRD2 and BRD3 proteins. Significantly, BD-9136 achieves strong inhibition of tumor growth in mice without any sign of toxicity. Furthermore, the present study demonstrates that conformational control of the PROTAC degrader molecule in its linker and linking position can achieve exceptional degradation selectivity for BRD4 over BRD2 and BRD3 proteins and suggests a strategy for the design of selective degraders for other proteins of interest.

■ **RESULTS**

Design of a Highly Selective BRD4 Degrader through Precise Conformational Control of the Linker and the Linking Position. We designed and synthesized a PROTAC degrader (**2**) by tethering our previously reported pan BET

inhibitor, QCA276 (**1**) with pomalidomide through a flexible, ethylamino linkage (Figure 1, Figure S1 and Table S1).[25] Compound **2** was tested for its ability to reduce BRD2, BRD3, and BRD4 proteins in the MV4;11 leukemia cell line, which expresses high levels of each of these 3 BRD proteins. Compound **2** effectively degrades BRD2, BRD3, and BRD4 proteins in the MV4;11 cell line in a dose-dependent manner with a 4 h treatment time and achieves DC_{50} values of 0.5, 0.5, and 0.2 nM for BRD2, BRD3, and BRD4 proteins, respectively (Table 1). The maximum degradation (D_{max}) values achieved by compound **2** against BRD2, BRD3, and BRD4 are all >95% (Table 1, Figure S1, and Table S1). Hence, compound **2** is a potent and effective but nonselective degrader of these three BET members.

Table 1. Degradation Potency and Selectivity of Compounds 1−8 against BRD2, BRD3, and BRD4 in the MV4;11 Cell Line[a]

ID	MV4;11 cell (4 h treatment time)					
	BRD2		BRD3		BRD4	
	DC_{50} (nM)	D_{max} (%)	DC_{50} (nM)	D_{max} (%)	DC_{50} (nM)	D_{max} (%)
1 (QCA276)	>1000	0	>1000	0	>1000	0
2 (BD-764)	0.5	99	0.5	98	0.2	98
3 (BD-7102)	0.3	97	0.4	98	0.1	98
4 (BD-7163)	50	68	>100	56	0.4	98
5 (BD-7148)	>1000	0	>1000	0	0.9	99
6 (BD-7162)	0.2	99	0.7	99	0.3	98
7 (BD-7181)	>1000	5	>1000	12	>1000	2
8 (BD-9136)	>1000	0	>1000	0	1.2	99

[a]Cells were treated for 4 h with each compound at different concentrations for Western blotting analysis of BRD2, BRD3, and BRD4 proteins with GAPDH used as the loading control. DC_{50}, which is the concentration that reduces 50% of the protein level over the control treatment, was calculated from the quantification of western blots. D_{max} indicates the maximum level of protein reduction.
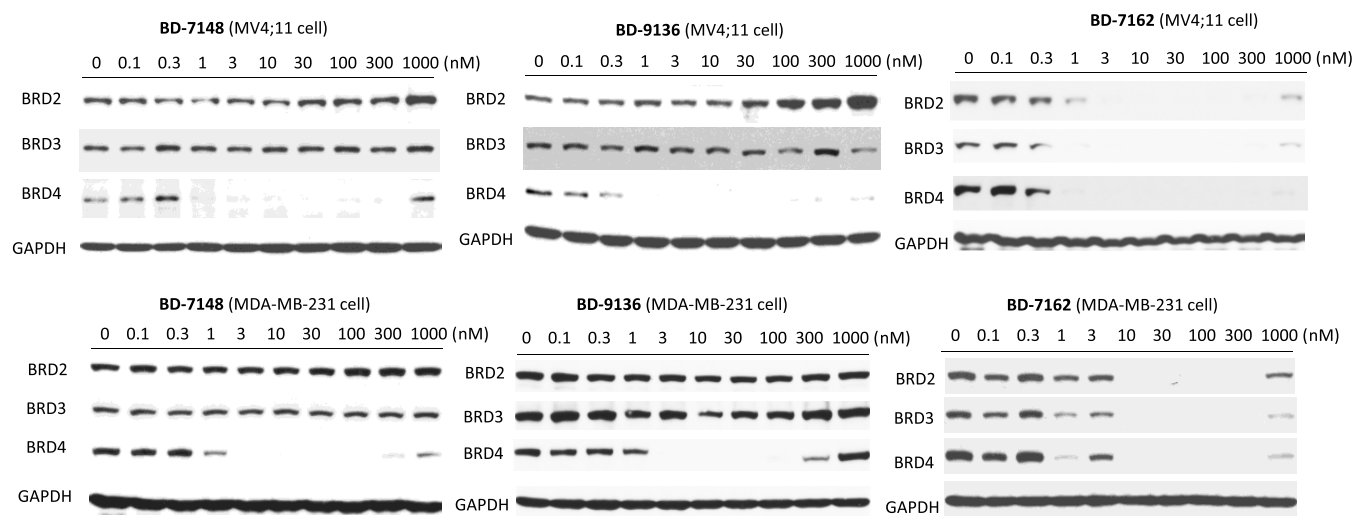
Figure 2. Western blot analysis of BRD2, BRD3, and BRD4 proteins in the in MV4;11 and MDA-MB-231 cells treated with BD-7148, BD-7162, and BD-9136. Cells were treated with indicated compounds at different concentrations for 4 h for western blotting analysis of BRD2, BRD3, and BRD4 proteins with GAPDH included as the loading control.

We replaced the flexible ethylamino linker in **2** with a semirigid methylazetidine linker, obtaining compound **3** (Figure 1), which was found to have DC$_{50}$ values of 0.3, 0.4, and 0.1 nM against BRD2, BRD3, and BRD4 proteins, respectively (Table 1, Figure S1, and Table S1). Hence, similar to compound **2**, compound **3** is also a potent but nonselective degrader against BRD2, BRD3, and BRD4 proteins.

We next synthesized compound **4** (Figure 1) using a piperidinyl group, which has no freely rotatable bonds in the linker thus restricting the linker conformation. Compound **4** achieves a DC$_{50}$ value of 0.4 nM and D_{max} = 98% against BRD4 but displays a selectivity of >100-fold for BRD4 over BRD2 and BRD3, in the MV4;11 cell line (Table 1, Figure S1, and Table S1).

Excited by the BRD4 degradation selectivity achieved with compound **4**, we replaced the piperidinyl group in the linker with an azetidinyl group, which is shorter and more rigid than the piperidinyl group, yielding compound **5** (BD-7148) (Figure 1). BD-7148 has DC$_{50}$ = 0.9 nM and D_{max} = 99% against BRD4 but no significant effect on the levels of BRD2 and BRD3 proteins at concentrations up to 1000 nM (Table 1, Figure 2, Figure S1, and Table S1). Hence, BD-7148 displays >1000-fold degradation selectivity for BRD4 over both BRD2 and BRD3.

We investigated if the position of the linker to the cereblon ligand in BD-7148 is critical in its high selectivity for the degradation of BRD4 over BRD2 and BRD3. For this purpose, we changed the tethering position of the azetidinyl group from the 4-position of the cereblon ligand in BD-7148 to the 5-position, thus generating compound **6** (BD-7162) (Figure 1), which shows a DC$_{50}$ value of 0.3 nM against BRD4 in the MV4;11 cell line (Table 1, Figure 2, Figure S1, and Table S1). In sharp contrast to BD-7148, BD-7162 also effectively and potently degrades BRD2 and BRD3 proteins with DC$_{50}$ values of 0.2 and 0.7 nM, respectively, in the MV4;11 cell line. Hence, BD-7162 is a highly potent but nonselective degrader of BRD2, BRD3, and BRD4 proteins.

To determine if the selective BRD4 degradation could be due to selective binding to BRD4, we determined the binding affinities of the BET inhibitor (**1**), and the degraders (**2**, **5**, and **6**) to BRD2-BRD4 BD1 and BD2 proteins (Table 2, Figure

Table 2. Binding Affinities of BET Inhibitor and Degraders to Recombinant Human BRD2, BRD3 and BRD4 BD1 and BD2 Domain Proteins as Determined by the Biolayer Interferometry (BLI) Assay Performed in Triplicates

protein	binding affinities K_d (nM)			
	1 (QCA276)	**2** (QCA764)	**5** (BD-7148)	**6** (BD-7162)
BRD2 BD1	120 ± 19	140 ± 11	39 ± 7.5	8.3 ± 2.3
BRD2 BD2	680 ± 210	350 ± 15	230 ± 25	110 ± 19
BRD3 BD1	73 ± 8.5	93 ± 14	46 ± 6.3	14 ± 2.6
BRD3 BD2	180 ± 37	160 ± 56	26 ± 4.1	26 ± 8
BRD4 BD1	35 ± 4.3	32 ± 8.4	66 ± 11	170 ± 41
BRD4 BD2	94 ± 31	71 ± 9.5	240 ± 38	210 ± 8.5

S2). Our binding data showed that the inhibitor (**1**) binds to each of these 6 recombinant human proteins with slightly better affinities to BD1 proteins than to the corresponding BD2 proteins. However, the inhibitor (**1**) displays a very modest selectivity for BDR4 BD1 over the BRD2 BD1 and BRD3 BD1 proteins. The degrader (**2**) has a very similar binding affinity to each of these BRD proteins compared to that for the inhibitor **1**. The degrader (**5**, BD-7148) shows similar binding affinities to BRD2 BD1, BRD3 BD1, BRD3 BD2, and BRD4 BD2 proteins. Degrader **6** binds to BRD2 BD1, BRD3 BD1, and BRD3 BD2 proteins with similar affinities and weaker affinities to BRD2 BD2, BRD4 BD1, and BRD4 BD2 proteins. Taken together, our binding data clearly show that the highly selective degradation of BRD4 protein over BRD2 and BRD3 proteins by degrader **5** (BD-7148) is not due to its selective binding to BRD4 BD1 or BD2 proteins over BRD2 or BRD3 BD1 and BD2 proteins.

Installation of a methyl group onto the piperidine-2,6-dione in compound **7** disrupts the hydrogen-bonding interaction between cereblon ligand and cereblon and reduces the binding of cereblon ligand to cereblon.[31] A methyl group was thus installed onto the piperidine-2,6-dione in BD-7148 to form compound **7** (BD-7181) as a control. As expected, compound **7** at all concentrations evaluated fails to induce degradation of BRD4, as well as BRD2 and BRD3 proteins (Table 1), indicating that the binding of BD-7148 to cereblon is necessary for its ability to induce BRD4 degradation.

We investigated the degradation mechanism of BD-7148 by chemical rescue experiments (Figure S3), and our results showed that QCA276 and pomalidomide completely block the BRD4 degradation induced by BD-7148. Carfilzomib, a selective proteasome inhibitor, and MLN4924, a neddylation inhibitor, also effectively block BRD4 degradation by BD-7148. Hence, BRD4 degradation by BD-7148 requires its binding to BRD4 and the cereblon/cullin 4A E3 ligase complex, and is proteasome- and neddylation-dependent, confirming that BD-7148 functions as a *bona fide* PROTAC BRD4 degrader.

Evaluation of BD-7148 in Additional Leukemia and Breast Cancer Cell Lines for Degradation Potency and Selectivity. To examine if the selective BRD4 degradation by BD-7148 is restricted to the MV4;11 cell line, we evaluated BD-7148 in three additional human acute leukemia cell lines to further define its degradation potency and selectivity on these BET proteins and obtained the data summarized in Table 3 and Figure 2 with additional details in Figure S4 and Table S2.

Table 3. Degradation Potencies of BD-7148 against BRD2, BRD3, and BRD4 in 3 Additional Human Leukemia and 4 Human Cancer Cell Lines[a]

compound ID	BD-7148					
	BRD2		BRD3		BRD4	
	DC_{50} (nM)	D_{max} (%)	DC_{50} (nM)	D_{max} (%)	DC_{50} (nM)	D_{max} (%)
RS4;11	>1000	<10	>1000	6	0.2	93
HL60	>1000	10	>1000	18	3.6	93
MOLM13	>1000	27	>1000	13	13	92
MDA-MB-231	>1000	0	>1000	19	1.0	93
MDA-MB-453	>1000	18	>1000	5	5.6	95
MCF-7	>1000	0	>1000	34	3.5	90
T47D	>1000	0	>1000	22	0.2	95

[a]Cells were treated for 4 hours with BD-7148 at different concentrations for Western blotting analysis of BRD2, BRD3 and BRD4 Proteins with GAPDH used as the loading control. DC_{50} was calculated from the quantification of western blots. D_{max} indicates the maximum level of protein reduction.

BD-7148 effectively and potently induces degradation of BRD4 protein, achieving DC_{50} values of 0.2, 3.6, and 13 nM in the RS4;11, HL-60, and MOLM13 acute leukemia cell lines, respectively, and a D_{max} of >90% in each of these leukemia cell lines. BD-7148 has a minimal effect on the levels of BRD2 and BRD3 proteins at concentrations up to 1000 nM, the highest concentration evaluated in these 3 cell lines.

We further evaluated BD-7148 in 4 human breast cancer cell lines, obtaining the data summarized in Table 3. BD-7148 is also highly potent and effective in inducing degradation of BRD4 protein and achieves DC_{50} values of 1, 5.6, 3.5, and 0.2 nM, respectively, in the MDA-MB-231, MDA-MB-453, MCF-7, and T47D cell lines, with D_{max} > 90% in each cell line. BD-7148 has little or no effect on the levels of BRD2 and BRD3 proteins up to 1000 nM.

Collectively, these data show that BD-7148 is a highly potent and effective BRD4 degrader and has >1000-fold selectivity over BRD2 and BRD3 proteins in all tested cell lines.

Design of BD-9136 as a More Soluble Analogue of BD-7148 for *In Vivo* Investigation. Although BD-7148 is a potent and highly selective BRD4 degrader, it has poor aqueous solubility, and this limits its evaluations in animals. To overcome this significant limitation, we installed a 4-methyl-piperazine-1-ethyl soluble group onto the bridging carbon of the azetidinyl group in BD-7148, obtaining compound **8** (BD-9136, Figure 1).

We evaluated the degradation potency of BD-9136 against BRD2, BRD3, and BRD4 proteins in these leukemia and breast cancer cell lines, and the resulting data are summarized in Table 4, and Figure 2 with additional details presented in Figure S5 and Table S3.

Table 4. Degradation Potencies of BD-9136 against BRD2, BRD3 and BRD4 in 4 Human Leukemia and 4 Human Breast Cancer Cell Lines[a]

ID	BD-9136					
	BRD2		BRD3		BRD4	
	DC_{50} (nM)	D_{max} (%)	DC_{50} (nM)	D_{max} (%)	DC_{50} (nM)	D_{max} (%)
MV-4-11	>1000	0	>1000	0	4.7	96
MOLM13	>1000	0	>1000	9	1.5	90
HL60	>1000	18	>1000	10	0.5	99
RS4;11	>1000	15	>1000	15	0.7	99
MDA-MB-231	>1000	0	>1000	0	0.5	95
MDA-MB-453	>1000	0	>1000	14	0.6	99
MCF-7	>1000	11	>1000	0	<0.1	99
T47D	>1000	6	>1000	25	0.2	99

[a]Cells were treated for 4 hours with BD-9136 at different concentrations for Western blotting analysis of BRD2, BRD3 and BRD4 Proteins with GAPDH used as the loading control. DC_{50} was calculated from the quantification of western blots. D_{max} indicates the maximum level of protein reduction.

BD-9136 is very potent and effective in inducing BRD4 degradation and achieves DC_{50} values of 0.1−4.7 nM and D_{max} of >90% in 8 cancer cell lines that were evaluated (Table 4). It is ineffective in inducing the degradation of BRD2 and BRD3 proteins in each of these 8 cancer cell lines at concentrations up to 1000 nM, the highest concentration evaluated. Hence, similar to BD-7148, BD-9136 demonstrates a high degradation potency against BRD4 protein and a clear selectivity over BRD2 and BRD3 proteins in each of these 8 cancer cell lines evaluated.

Evaluation of BD-7148 and BD-9136 for Cell Growth Inhibition in Leukemia and Breast Cancer Cell Lines. We evaluated the ability of BD-7148 and BD-9136 to inhibit cell growth in these 8 cancer cell lines, with QCA276, a pan BET inhibitor included as the control. The data are summarized in Table 5 and Figure S6.

BD-7148 potently and effectively inhibits cell growth in these leukemia and breast cancer cell lines, achieving IC_{50} values of 3.3−59.9 nM. In comparison, while QCA276 is effective in the inhibition of cell growth in each of these cancer cell lines, it is 8−189 times less potent than BD-7148.

BD-9136 is also potent and effective in the inhibition of cell growth, achieving DC_{50} values of 3.8−80.9 nM. In comparison, BD-9136 is slightly less potent than BD-7148 in each of these 8 cancer cell lines. BD-9136 is 3−164 times more potent than QCA276 in inhibition of cell growth in these 8 cancer cell lines.

Hence, the selective BRD4 degraders BD-7148 and BD-9136 are more potent than the pan BET inhibitor QCA276 in each of these 8 human cancer cell lines.

Table 5. Cell Growth Inhibition of QCA276, BD-7148, and BD-9136 in Leukemia and Breast Cancer Cell Lines[a]

cell lines	cell type	QCA276	BD-7148	potency enhancement (BD-7148/QCA276)	BD-9136	potency enhancement (BD-9136/QCA276)
				IC$_{50}$ (nM)		
MV4;11	AML	149 ± 12	17 ± 12	9	11 ± 3	14
MOLM13	AML	212 ± 39	25 ± 1.8	8	69 ± 6.2	3
HL60	AML	113 ± 8.9	4.9 ± 1.4	23	5.1 ± 1.1	22
RS4;11	ALL	186 ± 19	6.4 ± 0.5	29	4.6 ± 0.24	40
MDA-MB-231	TNBC	151 ± 30	15.9 ± 2.2	9	17.6 ± 1.5	9
MDA-MB-453	TNBC	689 ± 49	59.9 ± 0.8	12	80.9 ± 5.3	9
MCF-7	ER+BC	804 ± 40	37.8 ± 5.8	21	38.4 ± 12.1	21
T47D	ER+BC	623 ± 75	3.3 ± 0.1	189	3.8 ± 0.4	164

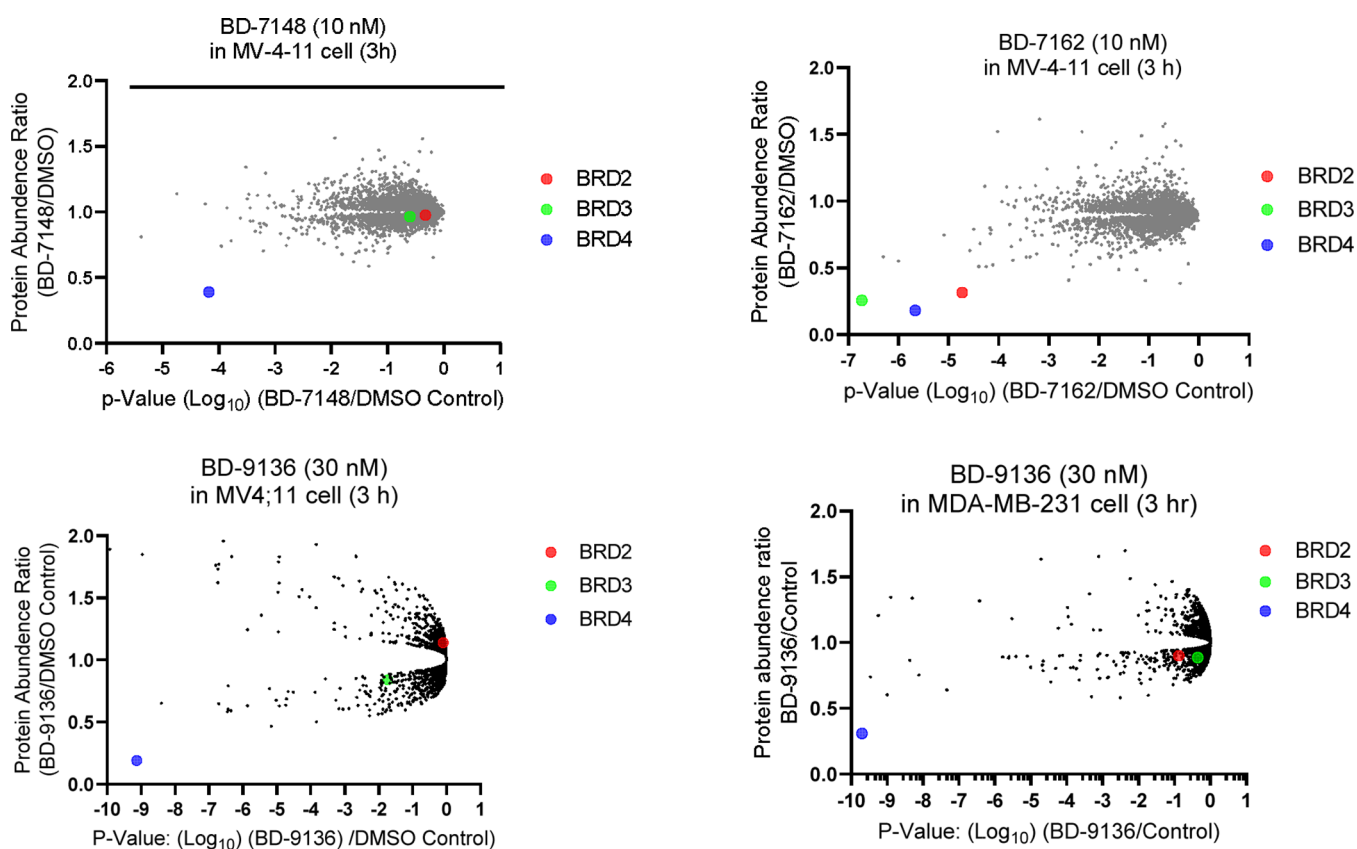[a]Cells were treated for 4 days, and cell viability was determined by WST-8 assay in triplicates.

Figure 3. Proteomic analysis of BRD4 selective and pan BET degraders in MV4;11 and MDA-MB-231 cell lines. Cells were treated with dimethyl sulfoxide (DMSO), BD-7148, or BD-9136 as indicated for proteomic analysis.

Proteomic Profiling of the Degradation Profiles of BRD4 Selective Degraders. We performed proteomic analysis of BD-7148 and BD-9136, two highly BRD4 selective degraders, and BD-7162, a nonselective BRD degrader for their degradation profiles in the whole proteasome in the MV4;11 cell line. The resulting data are summarized in Figure 3.

The results show that BD-7148 and BD-9136 reduce the level of BRD4 protein in the MV4;11 leukemia cell line but fail to significantly reduce >5,700 other proteins by a factor of more than 2. In comparison, BD-7162 reduces BRD2, BRD3, and BRD4 proteins in the MV4;11 cell line and does not significantly reduce >5700 other proteins by a factor of more than 2.

We further evaluated BD-9136 for its degradation selectivity profile in the MDA-MB-231 breast cancer cell line using proteomic analysis. Our data in Figure 3 show that similar to

the results obtained in the MV4;11 cell line, BD-9136 significantly reduces only the level of BRD4 protein in the MDA-MB-231 cell line and does not significantly reduce any of the other >5700 proteins, including BRD2 and BRD3 proteins by more than 2-fold.

Taken together, these proteomic data clearly show that both BD-7148 and BD-9136 selectively and effectively reduce the levels of BRD4 among >5700 proteins analyzed in the MV4;11 and/or MDA-MB-231 cell lines. In comparison, BD-7162 is a potent and selective degrader of BRD2, BRD3, and BRD4 proteins among >5700 proteins analyzed the MV4;11 cell line.

Evaluation of Ternary Complex Formation for Selective and Nonselective Degraders. For a PROTAC degrader molecule, the formation of a ternary complex with the protein of interest (POI) and the E3 ligase is critical for effective degradation of the POI. We reasoned that the
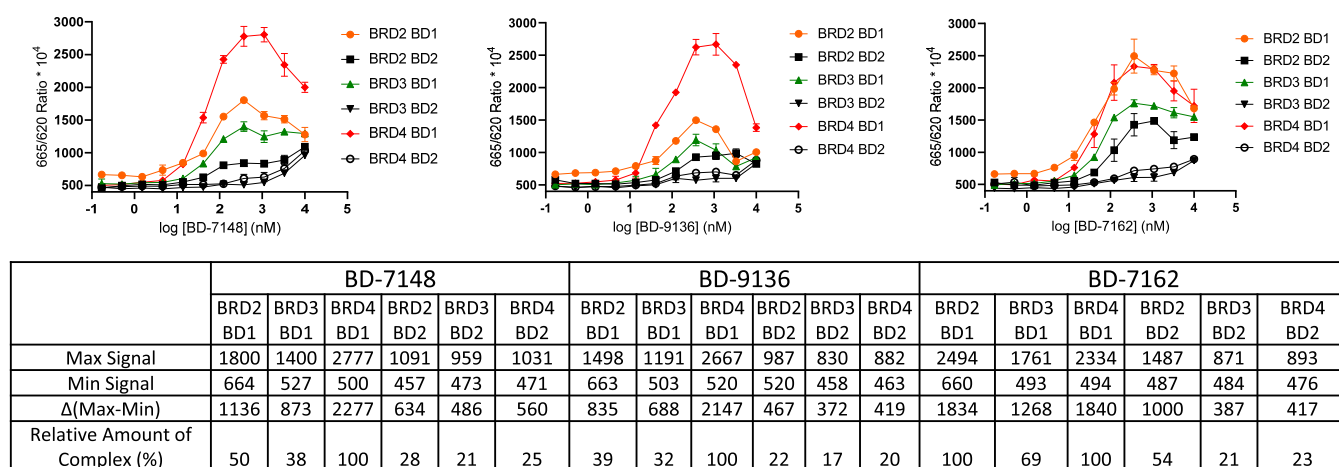
	BD-7148						BD-9136						BD-7162					
	BRD2 BD1	BRD3 BD1	BRD4 BD1	BRD2 BD2	BRD3 BD2	BRD4 BD2	BRD2 BD1	BRD3 BD1	BRD4 BD1	BRD2 BD2	BRD3 BD2	BRD4 BD2	BRD2 BD1	BRD3 BD1	BRD4 BD1	BRD2 BD2	BRD3 BD2	BRD4 BD2
Max Signal	1800	1400	2777	1091	959	1031	1498	1191	2667	987	830	882	2494	1761	2334	1487	871	893
Min Signal	664	527	500	457	473	471	663	503	520	520	458	463	660	493	494	487	484	476
Δ(Max-Min)	1136	873	2277	634	486	560	835	688	2147	467	372	419	1834	1268	1840	1000	387	417
Relative Amount of Complex (%)	50	38	100	28	21	25	39	32	100	22	17	20	100	69	100	54	21	23

Figure 4. Evaluation of ternary complex formation for BD-7148, BD-9136, BD-7162 with recombinant individual human BD1 and BD2 domains of BDR2, BRD3, and BRD4 proteins and recombinant human cereblon.
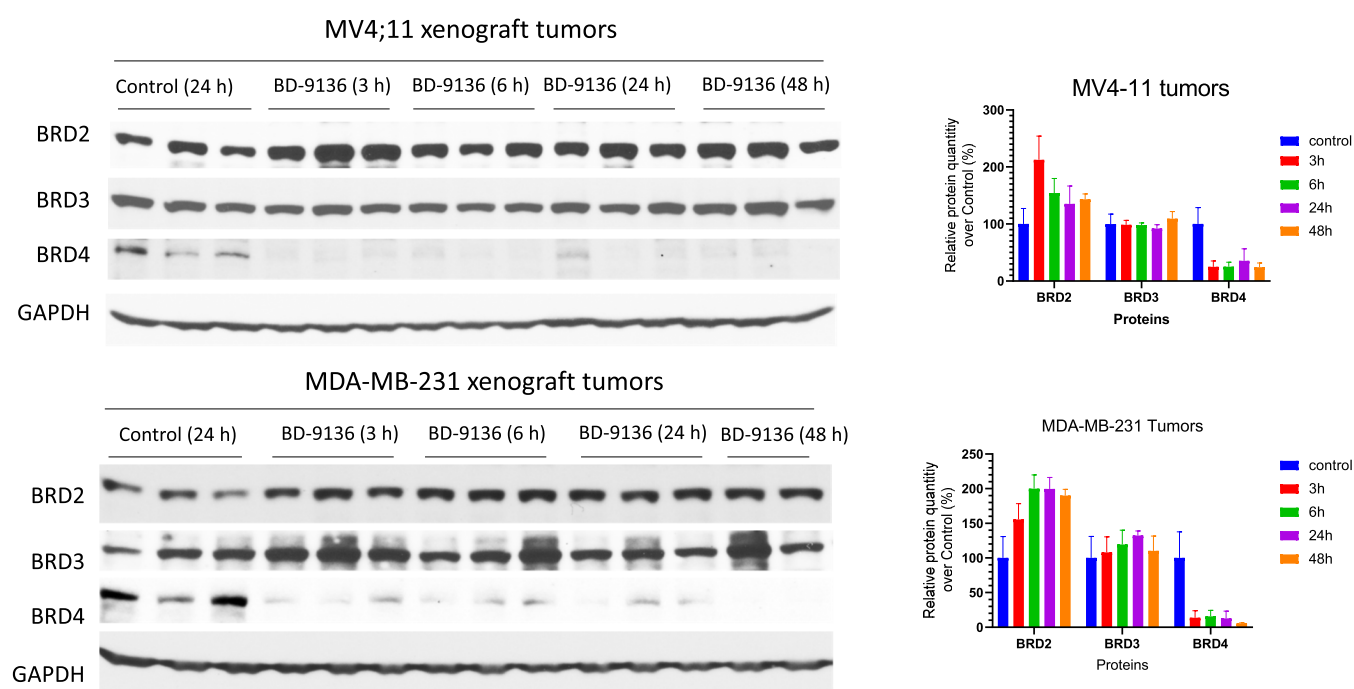
Figure 5. Pharmacodynamic analysis of BRD2, BRD3, and BRD4 proteins in the MV4;11 and MDA-MB-231 xenograft tumors in SCID mice. Mice bearing xenograft tumors were treated with a single administration of either vehicle control or BD-9136 at 20 mg/kg via intraperitoneal injection, and the mice were sacrificed at indicated time points. Tumor tissues were harvested for western blotting analysis.

exceptional selectivity achieved by BD-7148 and BD-9136 is due to, at least in part, their preferred formation of ternary complexes with BRD4 over BRD2 and BRD3 proteins. To test this hypothesis, we evaluated the formation of ternary complexes of BD-7148 and BD-9136 with recombinant human BD1 and BD2 proteins of BRD2, BRD3, and BRD4. We also evaluated BD-7162, a nonselective degrader in the ternary complex formation experiments. The data are summarized in Figure 4.

Our ternary complex formation data showed that while BD-7148 and BD-9136 are capable of forming ternary complexes with each of these six BD domain proteins, these two selective BRD4 degraders form the highest amount of ternary complex with BRD4 BD1 domain protein than with other BD domains. In comparison, the nonselective degrader BD-7162 forms the same amount of ternary complex for BRD2 BD1 and BRD

BD1 proteins and 31% less ternary complex with BRD3 BD1. Taken together, our data suggested that the exceptional degradation selectivity for BD-7148 and BD-9136 is due to, at least in part their ability to form preferred complexes with the BRD4 BD1 domain.

Pharmacodynamic Evaluation of BD-9136 in Mice. We evaluated the pharmacodynamics (PD) effect of BD-9136 *in vivo* in SCID mice bearing the MV4;11 and MDA-MB-231 xenograft tumors, with QCA276 included as the BET inhibitor control. The data are summarized in Figures 5 and S7.

Our data show that a single intraperitoneal (IP) injection of BD-9136 at 20 mg/kg significantly reduces the level of BRD4 protein over the vehicle control by 80, 87, and 70% at the 6, 24, and 48 time points, respectively, in the MV4;11 tumor tissue. BD-9136 has no significant effect on the levels of BRD3 protein at all of the time points examined but modestly
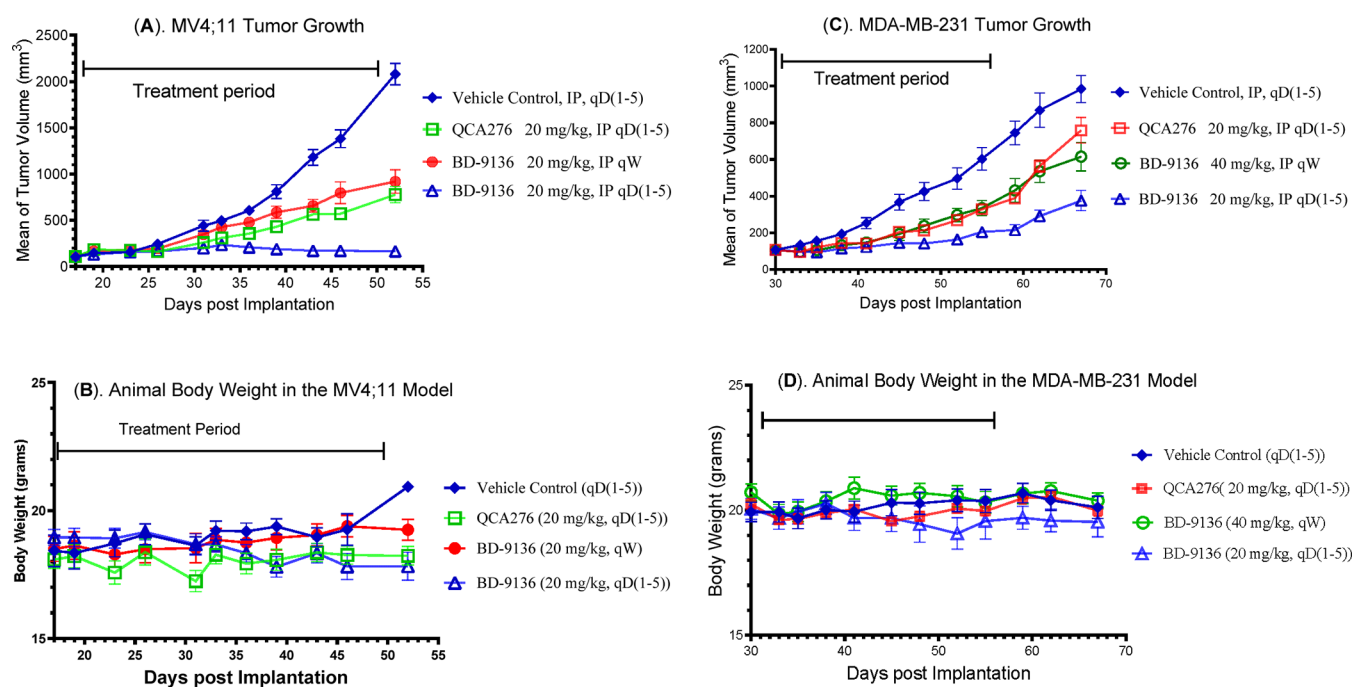
Figure 6. Antitumor activity of BD-9136 and QCA276 in the MV4;11 and MD-MB-231 xenograft models. SCID mice bearing MV4;11 or MDA-MB-231 xenograft tumors (one tumor per mouse) were treated with QCA276 or BD-9136 *via* intraperitoneal injection at indicated doses and schedules. Tumors were measured and animals were weighed twice a week. Each group consisted of 7 mice/tumors.

increases the levels of BRD2 protein in the MV4;11 tumor tissue at the 3 h time point.

Similar to the PD effect in the MV4;11 xenograft tumors, a single IP injection of BD-9136 at 20 mg/kg profoundly reduces the levels of BRD4 protein in the MDA-MB-231 tumor tissue as early as 3 h, and the effect persists for at least 48 h. BD-9136 has no significant effect on the levels of BRD3 protein between 3 and 48 h but modestly increases the levels of BRD2 protein in the MDA-MB-231 tumor tissues at all of the 4 time points examined.

In the MV4;11 tumors, treatment with QCA276, the BET inhibitor, has no significant reduction in the levels of BRD3 and BRD4 protein levels but modestly increases the levels of BRD2 protein (Figure S7). In the MDA-MB-231 tumors, treatment with QCA276 increases the levels of BRD2, BRD3, and BRD4 proteins at least in some of the time points examined (Figure S7).

Therefore, our PD data demonstrates that a single dose of BD-9136 effectively reduces the level of BRD4 protein in both the MV4;11 and MDA-MB-231 xenograft tumor tissues with the effect persisting for at least 48 h. Significantly, BD-9136 has no reduction in the levels of BRD2 and BRD3 proteins at all of the time points examined in both tumor models, demonstrating a high *in vivo* degradation selectivity.

Antitumor Activity of BD-9136 in Mice. Based upon the promising PD data, we assessed the antitumor activity of BD-9136 in the MV4;11 and MDA-MB-231 xenograft models, with QCA276 included as the control. The data are summarized in Figure 6.

In the MV4;11 model, QCA276 at a dosage of 20 mg/kg, 5 days a week for 4 weeks inhibited tumor growth by 63% at the end of the treatment ($p < 0.001$). In comparison, BD-9136 administered at 20 mg/kg, 5 days a week for 4 weeks achieved 92% of tumor growth inhibition at the end of the treatment. Because a single dose of BD-9136 reduces BRD4 in the tumor

tissue effectively for at least 48 h, we also evaluated BD-9136 with a weekly dosing. Our data showed that BD-9136 at 20 mg/kg, weekly administration inhibits tumor growth by 56%. In both of these two different dosing schedules, BD-9136 caused no significant weight loss or other signs of toxicity in mice during the entire experiment.

In the MDA-MB-231 xenograft tumor model, BD-9136 administered at 20 mg/kg, daily, 5 days per week inhibits tumor growth by 87% over the vehicle control group. In comparison, at the same dose and schedule, QCA276, the BET inhibitor, inhibits tumor growth by 49%. Thus, BD-9136 is much more effective in the inhibition of MDA-MB-231 tumor growth than its corresponding BET inhibitor, QCA276 at the same dose schedule. We further evaluated BD-9136 with weekly administration, and our data showed that weekly dosing of BD-9136 is as effective in the inhibition of tumor growth as QCA276 administered daily, 5 days a week. Both BD-9136 and QCA276 are well tolerated in mice in the MDA-MB-231 efficacy experiments.

◼ DISCUSSION AND CONCLUSIONS

One of the very attractive features of a PROTAC degrader molecule is its ability to achieve high degradation selectivity for one protein over its closely homologous proteins.[19,20,24,27,31−37] This is due to the fact that a PROTAC degrader must form a productive ternary complex consisting of the degrader itself, the protein of interest (POI), and an E3 ligase, to achieve effective degradation of the POI.[17] The formation of the productive ternary complex may involve protein surface residues from both the POI and the E3 ligase.[17,24,27] In contrast to the conserved binding site residues in homologous proteins, protein surface residues are not well conserved even among highly homologous proteins. The requirement of formation of a productive ternary complex by engaging less conserved surface residues, therefore, provides an

Scheme 1. Synthesis of Key Intermediate 19[a]
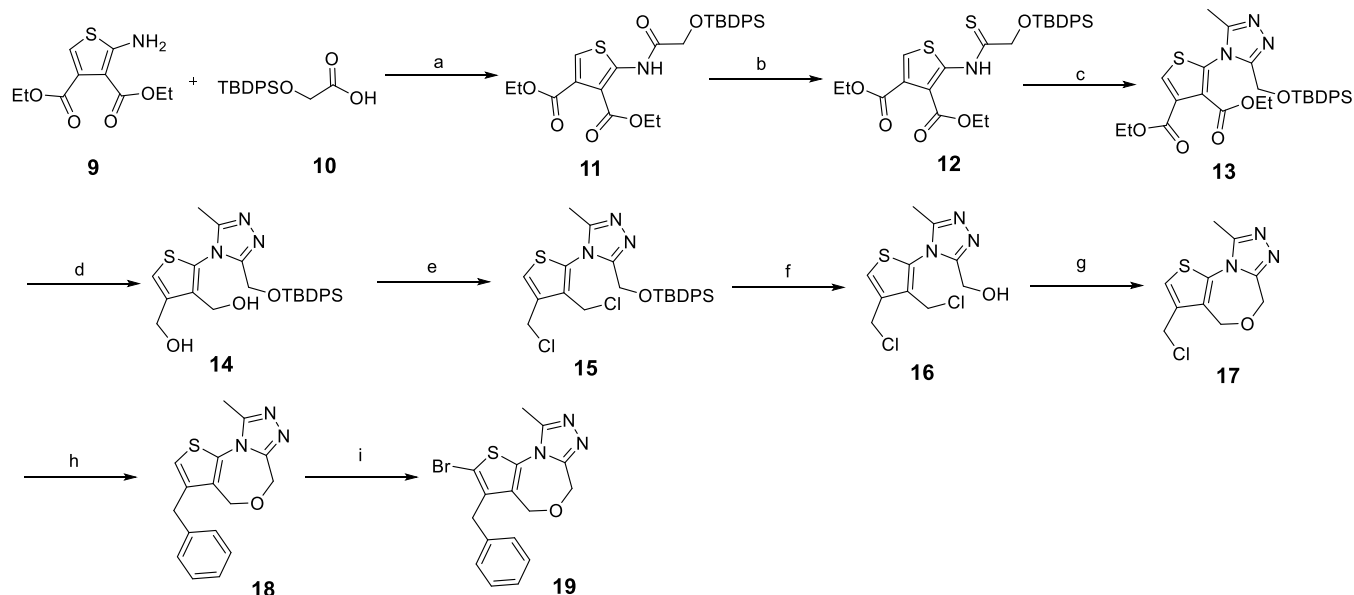
[a]Reagents and conditions: (a) (i) (COCl)$_2$, *N,N*-dimethylformamide (DMF), dichloromethane (DCM), 0 °C to room temperature (rt), 2 h; (ii) *N,N*-diisopropylethylamine (DIPEA), DCM, 1 h; 77% (b) Lawesson's reagent, dioxane, reflux, 4 h, 79%; (c) (i) NH$_2$NH$_2$·H$_2$O, tetrahydrofuran (THF), 0 °C to rt, 2 h; (ii) CH(OEt)$_3$, EtOH/THF, reflux, 2 h; (iii) AcOH, reflux, 2 h; 73% (d) LiBH$_4$, THF/MeOH (v/v 10:1), 0 °C to rt, 6 h; (e) SOCl$_2$, DCM, 0 °C to rt, 2 h; 55% over two steps; (f) tetra-*n*-butylammonium fluoride (TBAF), THF, 0 °C to rt, 2 h; (g) *t*-BuOK, *t*-BuOH, reflux, 10 min; 80% over two steps; (h) PhB(OH)$_2$, PdCl$_2$, PPh$_3$, Na$_2$CO$_3$, THF/H$_2$O (v/v 1:1), 60 °C, 6 h, 91%; (i) *N*-bromosuccinimide (NBS), AcOH, rt, 1 h, 90%.

opportunity to achieve high selectivity for the POI over its highly homologous proteins with appropriately designed PROTAC degrader molecules. In addition to selective BRD4 degraders,[20,24,27] the PROTAC technology has been used for the successful discovery of potent and selective degraders for a number of traditionally undruggable or difficultly druggable therapeutic targets.[31–33,35–37] We have previously reported the discovery of a highly selective and efficacious STAT3 PROTAC degrader using a modestly selective STAT3 ligand.[32,33] Two recent studies reported the discovery of selective SMARCA2 degraders over its close homologous SMARCA4 protein, which were designed using nonselective SMARCA2/4 ligands.[35,36] Using a ligand with no selectivity for STAT5 and STAT6 proteins, we recently reported our successful development of a potent, selective, and efficacious STAT5 PROTAC degrader over STAT6.[31,37] These studies highlight the power of the PROTAC technology to selectively target one protein over its highly homologous proteins.

In this study, we have demonstrated that starting from a nonselective pan BET inhibitor, highly potent BRD4 degraders with an exceptional degradation selectivity over BRD2 and BRD3 can be successfully developed through precise conformational control of the linker and the linking position on the cereblon ligand in the degrader molecule. Our data clearly demonstrate that a highly rigid linker is essential to achieve high degradation selectivity since the insertion of one additional methylene group into the linker converts an exceptionally selective BRD4 degrader into a completely nonselective, pan degrader against all of the three BRD proteins. Interestingly, switching the linking position from the 4-position of the phenyl ring to the 5-position also completely eliminates the BRD4 degradation selectivity over BRD2 and BRD3 proteins. Taken together, these results provide an elegant example of a precisely conformationally controlled

PROTAC degrader achieving exceptional selectivity for one protein over highly homologous proteins.

To gain mechanistic insights into the selective BRD4 degradation, we performed ternary complex formation assays using recombinant individual human BD1 and BD2 domain proteins for BRD2, BRD3, and BRD4 and recombinant human cereblon protein (Figure 4). Our data clearly showed that BD-7148 and BD-9136, two highly selective BRD4 degraders, form the highest amount of ternary complex with BRD4 BD1 over other BD domain proteins. In comparison, BD-7162, a nonselective degrader, forms the same amount of ternary complex with BRD2 and BRD4 BD1 proteins and a modestly less amount of ternary complex with BRD3 BD1 protein. These data shed light on the biochemical basis for the exceptional BRD4 degradation selectivity for BD-7148 and BD-9136. Of note, BD-7148 and BD-9136 are still capable of forming ternary complexes with other five BD domain proteins in our experiments. In fact, the maximum amount of the ternary complex formed for BD-7148 with BRD2 BD1 and BRD3 BD1 is 50% and 38% of that for BD-7148 with BRD4 BD1. It is very interesting to note that the 2- to 3-fold difference in the amount of ternary complexes formed between proteins can lead to exceptional degradation selectivity for one protein over their closely homologous proteins in cells.

Employing our highly potent and selective BRD4 degrader BD-7148 and its more soluble analogue BD-9136, we have demonstrated that selective BRD4 degradation leads to highly potent and effective cell growth inhibition in four human leukemia and four human breast cancer cell lines. In direct comparison, both BD-7148 and BD-9136 are more potent than their corresponding pan BET inhibitor, QCA276. We showed that selective and long-lasting BRD4 degradation can be successfully achieved in tumor tissues in mice with a single administration of a selective BRD4 degrader, BD-9136.

Significantly, BD-9136 is capable of achieving strong tumor growth inhibition in the MV4;11 and MDA-MB-231 xenograft models without any sign of toxicity and is more efficacious than the pan BET inhibitor, QCA276.

Although several selective BRD4 degraders have been reported previously, BD-7148 and BD-9136 are the most selective BRD4 degraders by achieving ≥1000-fold BRD4 degradation selectivity over BRD2 and BRD3. Our *in vivo* pharmacodynamic data also clearly demonstrated that a single dose of BD-9136 is highly effective in inducing near-complete and persistent depletion of BRD4 protein in tumor tissue, while having minimal or no effect on BRD2 and BRD3 proteins. While the functions of individual BRD proteins in gene regulation and human diseases are still under intense investigation, it is clear that while BRD proteins share some common functions, each BRD protein also has its own context-specific roles in gene regulation, biological processes, and consequently human diseases.[38] Therefore, a highly potent and exceptionally selective BRD4 degrader with strong *in vivo* activity such as BD-9136 is invaluable to investigate the therapeutic potential of selective BRD4 degradation for the treatment of human cancers and other human diseases. Importantly. This study has suggested a strategy for the design of potent and highly selective PROTAC degraders for one protein over its closely homologous proteins starting from a ligand with no selectivity between these homologous proteins.

◼ MATERIALS AND METHODS

Chemical Synthesis. Unless otherwise noted, all purchased chemical reagents and anhydrous solvents were used as received without further purification or drying. Experiments involving moisture- and/or air-sensitive components were performed in oven-dried glassware under an atmosphere of nitrogen or argon. Unless otherwise stated, all intermediates were purified by silica gel flash column chromatography eluting with either hexane in ethyl acetate or dichloromethane in methanol. All final compounds were purified by C18 reversed-phase preparative high-performance liquid chromatography (HPLC) column chromatography eluting with solvent A (0.1% trifluoroacetic acid (TFA) in water) and solvent B (0.1% TFA in acetonitrile) and were obtained as powders after lyophilization. Purified compounds were characterized by nuclear magnetic resonance (NMR) and ultraperformance liquid chromatography (UPLC)—mass spectrometry. ^{1}H NMR and ^{13}C NMR spectra were recorded on a Bruker Advance 400 MHz spectrometer. ^{1}H NMR spectra are reported in units of parts per million (ppm) downfield from tetramethylsilane (TMS). All ^{13}C NMR spectra were obtained with ^{1}H decoupling and are reported in ppm. In the spectral data reported, the format (δ) chemical shift (multiplicity, J values in Hz, integration) was used with the following abbreviations: s = singlet, d = doublet, t = triplet, q = quartet, m = multiplet. MS analyses were conducted with a Waters UPLC—mass spectrometer. The purities of all of the final compounds were determined to be over 95% by UPLC-MS analysis, which was monitored at 220 and 254 nm.

The synthesis of key intermediate **19** is shown in Scheme 1.

Step a: Diethyl 2-(2-((tert-Butyldiphenylsilyl)oxy)acetamido)-thiophene-3,4-dicarboxylate (11). Oxalyl chloride (2.0 equiv, 40 mmol, 3.4 mL) was added to a solution of 2-((*tert*-butyldiphenylsilyl)-oxy)acetic acid (**10**, 6.29 g, 20 mmol, 1.0 equiv) in DCM (60 mL) at 0 °C under N$_2$, and this was followed by the addition of DMF (0.1 mL). The mixture was warmed to ambient temperature and stirred for 1 h. All of the volatiles were removed *in vacuo*, and the residue was dissolved in DCM (10 mL). This solution was added to a solution of diethyl 2-aminothiophene-3,4-dicarboxylate (**9**, 4.38 g, 18 mmol, 0.9 equiv) in DCM (60 mL) and DIPEA (5.2 mL, 30 mmol) at 0 °C under N$_2$. The reaction mixture was warmed to ambient temperature and stirred for 1 h prior to being quenched with saturated NaHCO$_3$ (aq) and extracted with DCM (2 × 50 mL). The combined organic

layer was dried with Na$_2$SO$_4$, filtered, and concentrated. The residue was purified by silica gel flash chromatography and eluted with hexane/EtOAc (100:1−5:1) to give the title compound as a colorless oil (7.48 g, 77% yield). ^{1}H NMR (CDCl$_3$, 400 MHz) δ (ppm) 11.97 (s, 1H), 7.71−7.68 (m, 4H), 7.47−7.39 (m, 6H), 7.17 (s, 1H), 4.36−4.31 (m, 4H), 4.29 (s, 2H), 1.39−1.26 (m, 6H), 1.18 (s, 9H); UPLC-MS (ESI$^+$) calculated for C$_{28}$H$_{34}$NO$_6$SSi [M + H]$^+$: 540.19, found 540.37.

Step b: Diethyl 2-(2-((tert-Butyldiphenylsilyl)oxy)-ethanethioamido)thiophene-3,4-dicarboxylate (12). Lawesson's reagent (3.06 g, 7.57 mmol, 0.6 equiv) was added to a solution of compound **11** (6.8 g, 12.6 mmol, 1.0 equiv) in 1,4-dioxane (40 mL), and the reaction mixture was heated to reflux. The reaction was monitored by thin-layer chromatography (TLC), and all of the starting material was consumed within 4 h. The reaction mixture was cooled and diluted with EtOAc and water. After extraction, the combined organic layer was dried with Na$_2$SO$_4$, filtered, and concentrated. The residue was purified by silica gel flash chromatography eluting with hexane/EtOAc (100:1−5:1) to give the title compound as a colorless oil (5.71 g, 79% yield). ^{1}H (CDCl$_3$, 400 MHz) δ (ppm) 13.60 (s, 1H), 7.71−7.69 (m, 4H), 7.46−7.38 (m, 6H), 7.18 (s, 2H), 4.60 (s, 2H), 4.38−4.31 (m, 4H), 1.40−1.33 (m, 6H), 1.19 (s, 9H); ^{13}C (CDCl$_3$, 100 MHz) δ (ppm) 196.08, 165.04, 164.53, 148.86, 135.72, 132.04, 131.10, 130.28, 128.09, 119.42, 115.71, 71.47, 67.22, 61.65, 26.80, 19.31, 14.35, 14.33.

Step c: Diethyl 2-(3-(((tert-Butyldiphenylsilyl)oxy)methyl)-5-methyl-4H-1,2,4-triazol-4-yl)thiophene-3,4-dicarboxylate (13). Hydrazine monohydrate (1.1 g, 22 mmol, 2.2 equiv) was added to a solution of compound **12** (5.71 g, 10 mmol, 1.0 equiv) in THF (50 mL) at 0 °C, and the reaction mixture was warmed to ambient temperature. The solution was stirred for 2 h before being concentrated *in vacuo*. The residue was taken up into DCM and washed with brine. The organic layer was separated, dried, and concentrated. The residue was dissolved in EtOH (30 mL) and THF (8 mL). Triethyl orthoacetate (5.50 mL, 30.03 mmol, 3 equiv) was added. The reaction mixture was heated at reflux for 2 h. All volatiles were removed *in vacuo*, and the residue was dissolved in AcOH (10 mL). The solution was heated to reflux for 2 h prior to the removal of the solvent *in vacuo*. The residue was taken up into EtOAc and washed with saturated Na$_2$CO$_3$ (aq). The organic layer was washed with brine, dried, and concentrated. The residue was purified by silica gel flash chromatography eluting with hexane/EtOAc (100:1−1:100) to give the title compound as a colorless oil (4.23 g, 73% yield). ^{1}H (CDCl$_3$, 400 MHz) δ (ppm) 8.04 (s, 1H), 7.57−7.55 (m, 2H), 7.44−7.30 (m, 8H), 4.80 (d, J = 12.8 Hz, 1H), 4.66 (d, J = 12.8 Hz, 1H), 4.39 (q, J = 7.2 Hz, 2H), 4.11 (q, J = 7.2 Hz, 2H), 2.33 (s, 3H), 1.39 (t, J = 7.2 Hz, 3H), 1.05 (t, J = 7.2 Hz, 3H), 0.96 (s, 9H); ^{13}C (CDCl$_3$, 100 MHz) δ (ppm) 161.70, 161.32, 154.34, 153.93, 135.75, 135.52, 134.50, 133.24, 132.50, 132.08, 132.05, 131.96, 130.12, 129.97, 128.01, 127.90, 62.37, 61.88, 56.62, 26.85, 19.18, 14.29, 13.83, 10.80; UPLC-MS (ESI$^+$) calculated for C$_{30}$H$_{36}$N$_3$O$_5$SSi [M + H]$^+$: 578.21, found 578.47.

Step d: (2-(3-(((tert-Butyldiphenylsilyl)oxy)methyl)-5-methyl-4H-1,2,4-triazol-4-yl)thiophene-3,4-diyl)dimethanol (14). MeOH (4.0 mL) was added to a solution of compound **13** (4.23 g, 7.3 mmol, 1.0 equiv) in THF (40 mL) and LiBH$_4$ (2 M in THF, 14.6 mL, 29.2 mmol, 4 equiv) at 0 °C, and the reaction mixture was warmed to ambient temperature and stirred for 6 h. The solvent was removed *in vacuo*. The residue was dissolved in EtOAc and water. The aqueous layer was extracted with EtOAc twice, and the combined organic layer was dried over anhydrous Na$_2$SO$_4$. After filtration and concentration, the residue containing **14** was used in the next step without column purification. UPLC-MS (ESI$^+$) calculated for C$_{26}$H$_{32}$N$_3$O$_3$SSi [M + 1]$^+$: 494.19, found 494.29.

Step e: 4-(3,4-bis(Chloromethyl)thiophen-2-yl)-3-(((tert-butyldiphenylsilyl)oxy)methyl)-5-methyl-4H-1,2,4-triazole (15). The aforementioned crude residue (**14**) was dissolved in DCM (20 mL) and cooled to 0 °C. Thionyl chloride (2.65 mL, 36.5 mmol, 5.0 equiv) was added, and the reaction mixture was warmed to ambient temperature. After reaction for 2 h, all of the volatiles were removed,

Scheme 2. Synthesis of Degrader Compounds 5 (BD-7148), 6 (BD-7162), and 7 (BD-7181)[a]
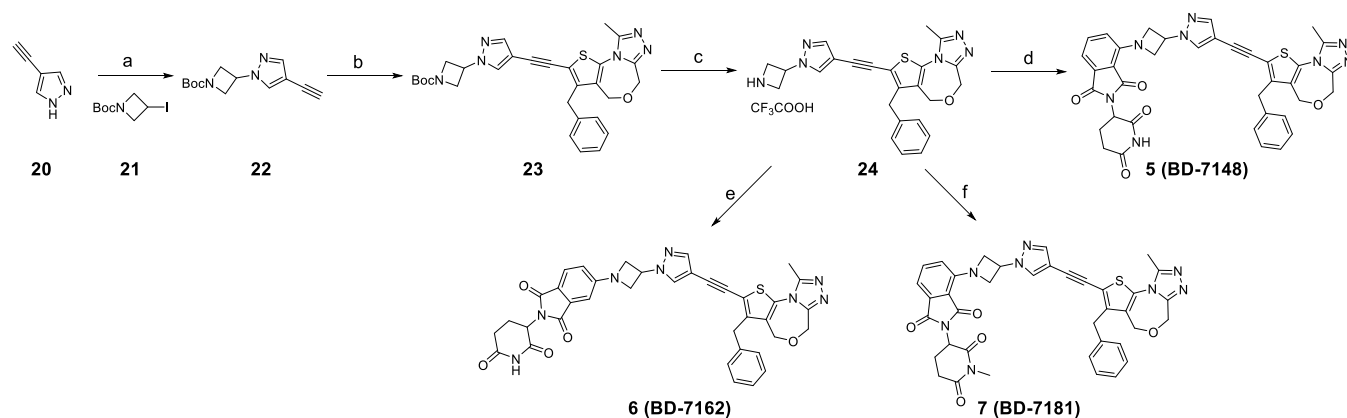
[a]Reagents and conditions: (a) Cs$_2$CO$_3$, DMF, 80 °C, 12 h, 89%; (b) **19**, Pd(PPh$_3$)$_2$Cl$_2$, CuI, DMF/trimethylamine (TEA) (v/v 1:1), 80 °C, 5 h, 85%; (c) DCM/TFA (v/v 2:1), rt, 1 h, 82%; (d) 2-(2,6-dioxopiperidin-3-yl)-4-fluoroisoindoline-1,3-dione, DIPEA, DMF, 90 °C, 12 h, 75%; (e) 2-(2,6-dioxopiperidin-3-yl)-5-fluoroisoindoline-1,3-dione, DIPEA, DMF, 90 °C, 12 h, 79%; (f) 4-fluoro-2-(1-methyl-2,6-dioxopiperidin-3-yl)isoindoline-1,3-dione, DIPEA, DMF, 90 °C, 12 h, 83%.

and the residue was taken up in EtOAc and washed with 2 M Na$_2$CO$_3$ (aq). The organic layer was washed with brine, dried, and concentrated. The residue was purified by silica gel flash chromatography eluting with hexane/EtOAc (100:1−2:1) to give the title compound as a white solid (2.12 g, 55% yield over two steps). UPLC-MS (ESI$^+$) calculated for C$_{26}$H$_{30}$Cl$_2$N$_3$OSSi [M + H]$^+$: 530.13, found 530.31.

Steps f, g: 3-(Chloromethyl)-9-methyl-4H,6H-thieno[2,3-e]-[1,2,4]triazolo[3,4-c][1,4]oxazepine (17). TBAF (4.0 mL, 4.0 mmol, 1.0 equiv, 1 M in THF) was added to a solution of compound **15** (2.12 g, 4.0 mmol, 1.0 equiv) in THF at 0 °C. The solution was stirred for 2 h before being added to a solution of potassium *tert*-butoxide (4.4 mL, 4.4 mmol, 1.1 equiv, 1.0 M in THF) in *tert*-butyl alcohol (20 mL) at 80 °C. The reaction mixture was stirred for 10 min prior to the removal of the solvent *in vacuo*. The residue was taken up in EtOAc and water. The organic layer was washed with brine, dried, and concentrated. The residue was purified by silica gel flash column chromatography eluting with hexane/EtOAc (100:1−1:100), then DCM/MeOH (100:1−10:1) to give the title compound as a colorless solid (818 mg, 80% yield over two steps). ^{1}H NMR (CDCl$_3$, 400 MHz) δ (ppm) 7.26 (s, 1H), 4.92 (s, 2H), 4.80 (s, 2H), 4.48 (s, 2H), 2.71 (s, 3H); ^{13}C (CDCl$_3$, 100 MHz) δ (ppm) 153.35, 150.88, 135.34, 132.27, 129.38, 121.25, 67.01, 62.52, 39.20, 12.72; UPLC-MS (ESI$^+$) calculated for C$_{10}$H$_{11}$ClN$_3$OS [M + H]$^+$: 256.03, found 256.19.

Step h: 3-Benzyl-9-methyl-4H,6H-thieno[2,3-e][1,2,4]triazolo-[3,4-c][1,4]oxazepine (18). PdCl$_2$ (44 mg, 0.25 mmol, 0.05 equiv) and PPh$_3$ (144 mg, 0.55 mmol, 0.11 equiv) were added to a solution of compound **17** (1.28 g, 5.0 mmol, 1.0 equiv) and phenylboronic acid (732 mg, 6.0 mmol, 1.2 equiv) in THF (15 mL). The solution was purged three times with nitrogen. Sodium carbonate (795 mg, 7.5 mmol, 1.5 equiv) was added in one portion, followed by injection of water (15 mL). The solution was purged with nitrogen another three times, and the resulting solution was stirred at 60 °C for 6 h. After cooling to room temperature (rt), the solution was diluted with EtOAc and water, followed by filtration through celite. The filtrate was transferred into a separatory funnel. The combined organic layer was dried over anhydrous sodium sulfate. After filtration, the solution was concentrated and the residue was purified by silica gel flash column chromatography eluting with hexane/EtOAc (10:1−1:100), then DCM/MeOH (100:1−10:1) to afford the desired compound as a colorless solid (1.36 g, 91% yield). UPLC-MS calculated for C$_{16}$H$_{16}$N$_3$OS [M + H]$^+$: 298.10, found 297.98.

Step i: 3-Benzyl-2-bromo-9-methyl-4H,6H-thieno[2,3-e][1,2,4]-triazolo[3,4-c][1,4]oxazepine (19). NBS (856 mg, 4.81 mmol, 1.05 equiv) was added to the compound obtained above (**18**, 1.36 g, 4.58 mmol, 1.0 equiv) in acetic acid (10 mL). The solution was stirred at

ambient temperature for 1−2 h. The reaction was mixed with saturated Na$_2$CO$_3$ (aq) slowly to neutralize the solution. The aqueous layer was extracted with EtOAc twice. The combined organic layer was dried over anhydrous Na$_2$SO$_4$. After filtration and concentration, the residue was purified by flash column chromatography with hexane/EtOAc (10:1−1:100) to afford the title compound as a colorless solid (1.54 g, 90% yield). UPLC-MS calculated for C$_{16}$H$_{15}$BrN$_3$OS [M + H]$^+$: 376.01, found 375.92.

3-Benzyl-9-methyl-2-((1-methyl-1H-pyrazol-4-yl)ethynyl)-4H,6H-thieno[2,3-e][1,2,4]triazolo-[3,4-c][1,4]oxazepine (1, QCA276) and 4-((2-(4-((3-Benzyl-9-methyl-4H,6H-thieno[2,3-e][1,2,4]triazolo[3,4-c][1,4]oxazepin-2-yl)ethynyl)-1H-pyrazol-1-yl)ethyl)amino)-2-(2,6-dioxopiperidin-3-yl)isoindoline-1,3-dione (2). The synthesis details and characterization of compound **1** and compound **2** have been described previously.[25] Compound **1** (**QCA276**): ^{1}H NMR (400 MHz, CD$_3$OD) δ (ppm) 7.87 (s, 1H), 7.63 (s, 1H), 7.30−7.27 (m, 2H), 7.23−7.18 (m, 3H), 4.73 (s, 2H), 4.71 (s, 2H), 4.07 (s, 2H), 3.89 (s, 3H), 2.78 (s, 3H); ^{13}C NMR (100 MHz, CD$_3$OD) δ (ppm) 155.41, 153.18, 143.28, 142.76, 139.44, 135.21, 132.68, 129.92, 129.80, 129.33, 127.77, 119.38, 103.27, 90.26, 81.43, 69.18, 62.71, 39.17, 34.68, 12.39.

The synthesis of degrader compounds **5** (BD-7148), **6** (BD-7162), and **7** (BD-7181) is provided in Scheme 2.

Step a: tert-Butyl 3-(4-Ethynyl-1H-pyrazol-1-yl)azetidine-1-carboxylate (22). Cesium carbonate (2.61 g, 8.0 mmol, 1.0 equiv) was added to a solution of 4-ethynyl-1*H*-pyrazole (**20**, 737 mg, 8.0 mmol, 1.0 equiv) and *tert*-butyl 3-iodoazetidine-1-carboxylate (**21**, 2.32 g, 8.2 mmol, 1.02 equiv) in DMF (20 mL). The solution was stirred at 80 °C for 12 h. After cooling to rt, the solution was diluted with EtOAc and filtered through celite. The filtrate was washed with saturated brine. The combined organic layer was dried over anhydrous sodium sulfate. After filtration and concentration, the residue was purified by silica gel flash column chromatography eluting with hexane/EtOAc (100:1−2:1) to afford the title compound as a white solid (1.77 g, 89% yield). ^{1}H NMR (400 MHz, CDCl$_3$) δ (ppm) 7.68 (s, 2H), 5.03−4.97 (m, 1H), 4.39−4.34 (m, 2H), 4.30−4.26 (m, 2H), 3.02 (s, 1H), 1.45 (s, 9H); ^{13}C NMR (100 MHz, CDCl$_3$) δ (ppm) 156.17, 143.32, 131.90, 103.05, 80.35, 78.76, 74.76, 56.55, 50.40, 28.47.

Step b: tert-Butyl 3-(4-((3-Benzyl-9-methyl-4H,6H-thieno[2,3-e][1,2,4]triazolo[3,4-c][1,4]-oxazepin-2-yl)ethynyl)-1H-pyrazol-1-yl)azetidine-1-carboxylate (23). Compound **22** (148 mg, 0.6 mmol, 1.2 equiv) was added to a solution of compound **19** (188 mg, 0.5 mmol, 1.0 equiv), Pd(PPh$_3$)$_2$Cl$_2$ (35 mg, 0.05 mmol, 0.1 equiv), and CuI (19 mg, 0.1 mmol, 0.2 equiv) in DMF (3.0 mL). The solution was purged three times with nitrogen under sonication. After injection of triethylamine (3.0 mL), the solution was purged and refilled with nitrogen three times under sonication The solution was stirred at 80

Scheme 3. Synthesis of Degrader Compound 8 (BD-9136)[a]
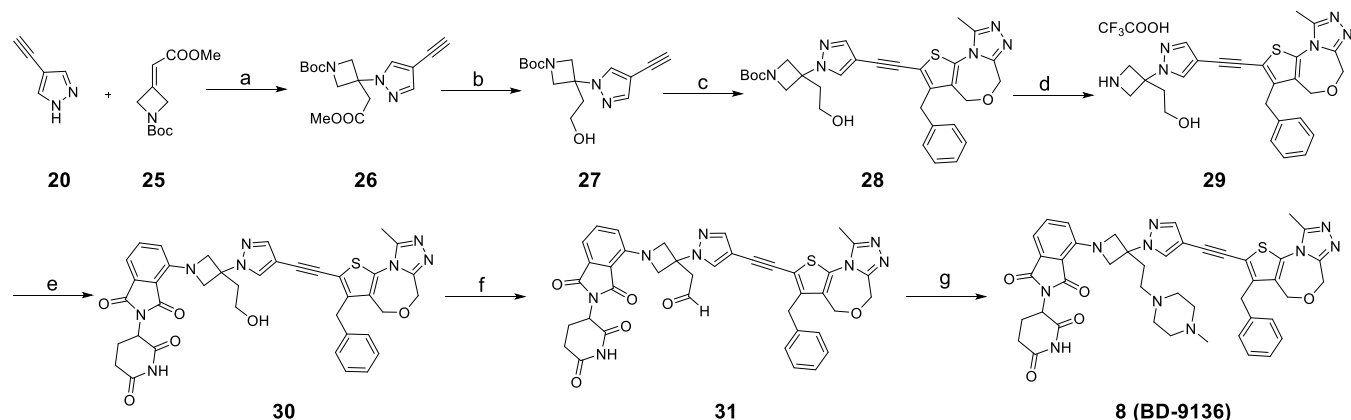
[a]Reagents and conditions: (a) DBU, MeCN, 70 °C, 12 h, 90%; (b) LiBH₄, MeOH/THF (v/v 1:7), 0 °C to rt, 2 h, 95%; (c) 19, Pd(PPh₃)₂Cl₂, CuI, DMF/TEA (v/v 3:2), 80 °C, 5 h, 92%; (d) (i) DCM/TFA (v/v 4:1), 0 °C to rt, 2 h; (ii) Na₂CO₃, MeCN/H₂O (v/v 1:2), 60 °C, 2 h; (e) 2-(2,6-dioxopiperidin-3-yl)-4-fluoroisoindoline-1,3-dione, DIPEA, DMF, 90 °C, 12 h; 74% over two steps; (f) Dess−Martin periodinane (DMP), DCM, RT, 6 h, 95%; (g) 1-methylpiperazine, NaBH(OAc)₃, 1,2-dichloroethane (DCE), 12 h, 83%.

°C for 5 h under nitrogen. After cooling to rt, the solution was diluted in EtOAc and saturated ammonium chloride. The aqueous layer was extracted with EtOAc twice. The combined organic layer was dried, filtrated, and concentrated. The residue was purified by silica gel flash column chromatography eluting with hexane/EtOAc (100:1-1:100), followed by DCM/MeOH (100:1−10:1) to afford the title compound as a brown oil (231 mg, 85% yield).

Step c: 2-((1-(Azetidin-3-yl)-1H-pyrazol-4-yl)ethynyl)-3-benzyl-9-methyl-4H,6H-thieno[2,3-e][1,2,4]triazolo[3,4-c][1,4]oxazepine (24). The compound 23 (231 mg) obtained above was dissolved in a solution of DCM/TFA (v/v 4:2 mL). After 1 h, the solvent was evaporated to afford the crude residue, which was purified by preparative HPLC eluting with MeCN/water (0.1% TFA) to afford the title compound (195 mg, TFA salt, 82% yield) as a colorless solid.

Step d: 4-(3-(4-((3-Benzyl-9-methyl-4H,6H-thieno[2,3-e][1,2,4]-triazolo[3,4-c][1,4]oxazepin-2-yl)ethynyl)-1H-pyrazol-1-yl)azetidin-1-yl)-2-(2,6-dioxopiperidin-3-yl)isoindoline-1,3-dione (5, BD-7148). DIPEA (183 μL, 1.05 mmol, 3.0 equiv) was added to a solution of 2-(2,6-dioxopiperidin-3-yl)-4-fluoroisoindoline-1,3-dione (106 mg, 0.385 mmol, 1.1 equiv) and compound 24 (195 mg, 0.35 mmol, 1.0 equiv, TFA salt) in DMF (3.0 mL). The solution was stirred at 90 °C for 12 h. After cooling to rt, the solution was diluted with water and purified by preparative HPLC eluting with MeCN/water (0.1% TFA) to afford the title compound as a yellow solid (183 mg, 75% yield). ¹H NMR (400 MHz, acetone-d_6) δ (ppm) 9.88 (s, 1H), 8.26 (s, 1H), 7.79 (s, 1H), 7.62 (dd, J = 8.4 Hz, J = 6.8 Hz, 1H), 7.33−7.22 (m, 5H), 7.19 (dd, J = 6.8 Hz, J = 0.8 Hz, 1H), 6.89 (dd, J = 8.4 Hz, J = 0.8 Hz, 1H), 5.50−5.45 (m, 1H), 5.07 (dd, J = 12.4 Hz, J = 5.2 Hz, 1H), 4.82 (t, J = 8.8 Hz, 2H), 4.73 (s, 2H), 4.72 (s, 2H), 4.63−4.59 (m, 2H), 4.12 (s, 2H), 3.00−2.90 (m, 1H), 2.81−2.70 (m, 5H), 2.21−2.15 (m, 1H); ¹³C NMR (100 MHz, acetone-d_6) δ (ppm) 172.62, 170.12, 168.14, 167.73, 154.33, 152.06, 148.65, 143.13, 143.05, 139.38, 135.77, 134.92, 133.85, 131.33, 130.93, 129.56, 129.19, 127.42, 120.64, 117.24, 113.17, 112.66, 103.08, 89.51, 81.72, 68.42, 62.97, 61.54, 52.02, 50.02, 34.39, 31.99, 23.34, 12.64; UPLC-MS (ESI⁺) calculated for C₃₇H₃₁N₈O₅S [M + 1]⁺: 699.21, found 699.27.

Step e: 5-(3-(4-((3-Benzyl-9-methyl-4H,6H-thieno[2,3-e][1,2,4]-triazolo[3,4-c][1,4]oxazepin-2-yl)ethynyl)-1H-pyrazol-1-yl)azetidin-1-yl)-2-(2,6-dioxopiperidin-3-yl)isoindoline-1,3-dione (6, BD-7162). DIPEA (78 μL, 0.45 mmol, 3.0 equiv) was added to a solution of 2-(2,6-dioxopiperidin-3-yl)-5-fluoroisoindoline-1,3-dione (45 mg, 0.165 mmol, 1.1 equiv) and compound 24 (82 mg, 0.15 mmol, 1.0 equiv) in DMF (2.0 mL). The solution was stirred at 90 °C for 12 h. After cooling to rt, the solution was diluted with water and purified by preparative HPLC eluting with MeCN/water (0.1%TFA) to afford the title compound as a yellow solid (83 mg, 79% yield). ¹H NMR

(400 MHz, acetone-d_6) δ (ppm) 9.88 (s, 1H), 8.27 (d, J = 0.4 Hz, 1H), 7.81 (s, 1H), 7.67 (d, J = 8.0 Hz, 1H), 7.34−7.27 (m, 4H), 7.24−7.20 (m, 1H), 6.90 (d, J = 2.0 Hz, 1H), 6.80 (dd, J = 8.4 Hz, J = 2.0 Hz, 1H), 5.62−5.55 (m, 1H), 5.07 (dd, J = 12.8 Hz, J = 5.6 Hz, 1H), 4.75 (s, 2H), 4.74 (s, 2H), 4.66 (t, J = 8.4 Hz, 2H), 4.50 (dd, J = 12.8 Hz, J = 5.2 Hz, 2H), 4.12 (s, 2H), 3.01−2.91 (m, 1H), 2.82−2.73 (m, 5H), 2.21−2.15 (m, 1H); ¹³C NMR (100 MHz, acetone-d_6) δ (ppm) 172.66, 170.22, 168.36, 168.09, 155.98, 154.18, 151.60, 143.27, 143.06, 139.33, 135.31, 134.00, 131.21, 129.57, 129.18, 127.44, 125.51, 119.70, 117.4S, 115.72, 105.79, 103.12, 89.55, 81.72, 68.52, 62.86, 59.40, 51.96, 50.08, 34.39, 32.03, 23.44, 12.59; UPLC-MS (ESI⁺) calculated for C₃₇H₃₁N₈O₅S [M + 1]⁺: 699.21, found 699.35.

Step f: 4-(3-(4-((3-Benzyl-9-methyl-4H,6H-thieno[2,3-e][1,2,4]-triazolo[3,4-c][1,4]oxazepin-2-yl)ethynyl)-1H-pyrazol-1-yl)azetidin-1-yl)-2-(1-methyl-2,6-dioxopiperidin-3-yl)isoindoline-1,3-dione (7, BD-7181). DIPEA (52 μL, 0.3 mmol, 3.0 equiv) was added to a solution of 4-fluoro-2-(1-methyl-2,6-dioxopiperidin-3-yl)isoindoline-1,3-dione (30 mg, 0.11 mmol, 1.1 equiv) and compound 24 (55 mg, 0.1 mmol, 1.0 equiv) in DMF (2.0 mL). The solution was stirred at 90 °C for 12 h. After cooling to rt, the solution was diluted with water and purified by preparative HPLC eluting with MeCN/water (0.1% TFA) to afford the title compound as a yellow solid (59 mg, 83% yield). ¹H NMR (400 MHz, acetone-d_6) δ (ppm) 8.25 (s, 1H), 7.79 (s, 1H), 7.59 (dd, J = 8.4 Hz, J = 6.8 Hz, 1H), 7.33−7.27 (m, 4H), 7.24−7.20 (m, 1H), 7.18 (d, J = 6.8 Hz, 1H), 6.86 (d, J = 8.0 Hz, 1H), 5.49 (m, 1H), 5.08 (dd, J = 12.8 Hz, J = 5.6 Hz, 1H), 4.85−4.77 (m, 6H), 4.61 (dd, J = 9.6 Hz, J = 5.2 Hz, 2H), 4.12 (s, 2H), 3.07 (s, 3H), 3.01−2.87 (m, 2H), 2.83 (s, 3H), 2.77−2.66 (m, 1H), 2.18−2.11 (m, 1H); ¹³C NMR (100 MHz, acetone-d_6) δ (ppm) 172.19, 170.34, 168.15, 167.73, 154.33, 152.06, 148.56, 143.15, 142.98, 139.21, 135.75, 134.84, 133.90, 131.85, 130.12, 129.56, 129.17, 127.46, 120.61, 118.09, 113.19, 112.60, 102.96, 89.98, 81.59, 68.79, 62.64, 61.51, 52.03, 50.60, 34.37, 32.26, 27.04, 22.58, 12.48; UPLC-MS (ESI⁺) calculated for C₃₈H₃₃N₈O₅S [M + 1]⁺: 713.23, found 713.35.

4-(3-((4-((3-Benzyl-9-methyl-4H,6H-thieno[2,3-e][1,2,4]triazolo-[3,4-c][1,4]oxazepin-2-yl)ethynyl)-1H-pyrazol-1-yl)methyl)azetidin-1-yl)-2-(2,6-dioxopiperidin-3-yl)isoindoline-1,3-dione (3, BD-7102). Compound 3 was prepared as a yellow solid in a manner similar to that described for compound 5. ¹H NMR (400 MHz, acetone-d_6) δ (ppm) 9.88 (s, 1H), 8.13 (d, J = 0.4 Hz, 1H), 7.71 (d, J = 0.4 Hz, 1H), 7.55 (dd, J = 8.4 Hz, J = 6.8 Hz, 1H), 7.34−7.28 (m, 4H), 7.25−7.21 (m, 1H), 7.11 (d, J = 6.8 Hz, 1H), 6.77 (d, J = 8.4 Hz, 1H), 5.05 (dd, J = 12.8 Hz, J = 5.6 Hz, 1H), 4.73 (s, 2H), 4.72 (s, 2H), 4.56 (d, J = 7.2 Hz, 2H), 4.39−4.34 (m, 2H), 4.16−4.12 (m, 2H), 4.11 (s, 2H), 3.35−3.27 (m, 1H), 2.99−2.89 (m, 1H), 2.81−2.73 (m, 2H),

2.69 (s, 3H), 2.21−2.12 (m, 1H); ^{13}C NMR (100 MHz, DMSO-d_6) δ (ppm) 172.74, 169.97, 167.17, 166.46, 153.00, 150.49, 147.86, 141.78, 141.76, 138.22, 134.92, 133.73, 133.23, 129.70, 128.66, 128.19, 126.49, 119.90, 115.53, 111.77, 110.14, 100.70, 89.03, 80.84, 67.41, 61.86, 54.07, 48.63, 33.17, 30.94, 29.50, 22.09, 12.21; UPLC-MS (ESI$^+$) calculated for $C_{38}H_{33}N_8O_5S$ [M + 1]$^+$: 713.23, found 713.33.

4-(4-(4-((3-Benzyl-9-methyl-4H,6H-thieno[2,3-e][1,2,4]triazolo-[3,4-c][1,4]oxazepin-2-yl)ethynyl)-1H-pyrazol-1-yl)piperidin-1-yl)-2-(2,6-dioxopiperidin-3-yl)isoindoline-1,3-dione (4, BD−7163). Compound **4** was prepared as a yellow solid in a manner similar to that described for compound **5**. ^{1}H NMR (400 MHz, acetone-d_6) δ (ppm) 9.88 (s, 1H), 8.15 (s, 1H), 7.74−7.70 (m, 2H), 7.40 (d, J = 8.0 Hz, 1H), 7.37 (d, J = 7.2 Hz, 1H), 7.34−7.29 (m, 4H), 7.25−7.22 (m, 1H), 5.13 (dd, J = 12.8 Hz, J = 5.6 Hz, 1H), 4.72 (s, 4H), 4.53−4.45 (m, 1H), 4.12 (s, 2H), 3.95−3.92 (m, 2H), 3.17 (t, J = 11.6 Hz, 2H), 2.98−2.92 (m, 1H), 2.84−2.74 (m, 2H), 2.70 (s, 3H), 2.38−2.19 (m, 5H); ^{13}C NMR (100 MHz, acetone-d_6) δ (ppm) 172.62, 170.16, 168.04, 167.52, 154.10, 151.32, 150.98, 148.83, 142.11, 139.43, 136.47, 135.25, 132.11, 131.16, 130.92, 129.56, 129.20, 127.41, 124.66, 118.63, 117.46, 115.77, 102.28, 90.09, 81.39, 68.44, 62.97, 59.95, 51.10, 50.14, 34.40, 33.14, 32.01, 23.34, 12.64; UPLC-MS (ESI$^+$) calculated for $C_{39}H_{35}N_8O_5S$ [M + 1]$^+$: 727.25, found 727.40.

The synthesis of degrader compound **8** (BD-9136) is shown in Scheme 3.

Step a: tert-Butyl 3-(4-Ethynyl-1H-pyrazol-1-yl)-3-(2-methoxy-2-oxoethyl)azetidine-1-carboxylate (26). 1,8-Diazabicyclo[5.4.0]-undec-7-ene (3.0 mL, 20 mmol, 1.0 equiv) was added to a solution of 4-ethynyl-1H-pyrazole (**20**, 1.84 g, 20 mmol, 1.0 equiv) and *tert*-butyl 3-(2-methoxy-2-oxo-ethylidene)azetidine-1-carboxylate (**25**, 4.55 g, 20 mmol, 1.0 equiv) in MeCN (20 mL). The mixture was stirred at 70 °C for 12 h. After cooling to ambient temperature, the mixture was concentrated and the residue was purified by silica gel flash column chromatography eluting with hexane/EtOAc (20:1−2:1) to afford the title compound as a white solid (5.75 g, 90% yield). ^{1}H NMR (400 MHz, CDCl$_3$) δ (ppm) 7.81 (s, 1H), 7.62 (s, 1H), 4.38 (d, J = 9.6 Hz, 2H), 4.25 (d, J = 9.6 Hz, 2H), 3.62 (s, 3H), 3.21 (s, 2H), 3.00 (s, 1H), 1.44 (s, 9H); ^{13}C NMR (100 MHz, CDCl$_3$) δ (ppm) 169.73, 156.11, 142.98, 131.67, 102.78, 80.57, 78.63, 74.87, 60.01, 57.42, 52.13, 41.95, 28.41; UPLC-MS (ESI$^+$) calculated for $C_{16}H_{21}N_3NaO_4$ [M + Na]$^+$: 342.14, found 342.19.

Step b: tert-Butyl 3-(4-Ethynyl-1H-pyrazol-1-yl)-3-(2-hydroxyethyl)azetidine-1-carboxylate (27). Lithium borohydride (2.0 M in THF, 22.5 mL, 45.0 mmol, 2.5 equiv) was added slowly to a solution of compound **26** (5.75 g, 18 mmol, 1.0 equiv) in MeOH (10 mL) and tetrahydrofuran (50 mL) at 0 °C under a nitrogen atmosphere. The solution was warmed to ambient temperature and stirred for 2 h. Water (1.0 mL) was added dropwise to quench the reaction. The solvent was removed *in vacuo*, and the residue was diluted with EtOAc (50 mL) and water (50 mL). After extraction, the organic layer was separated and dried over anhydrous sodium sulfate. After filtration, the solution was concentrated and the residue was purified by silica gel flash column chromatography eluting with hexane/EtOAc (10:1−1:2) to afford the title compound as a colorless oil (4.98 g, 95% yield). ^{1}H NMR (400 MHz, CDCl$_3$) δ (ppm) 7.73 (s, 1H), 7.67 (s, 1H), 4.38 (d, J = 9.2 Hz, 2H), 4.25 (d, J = 9.2 Hz, 2H), 3.44 (t, J = 6.4 Hz, 2H), 3.03 (s, 1H), 2.31 (t, J = 6.4 Hz, 2H), 1.44 (s, 9H); ^{13}C NMR (100 MHz, CDCl$_3$) δ (ppm) 156.22, 142.88, 131.48, 102.98, 80.43, 78.86, 74.74, 60.01, 59.19, 58.41, 40.96, 28.45.

Step c: tert-Butyl 3-(4-((3-Benzyl-9-methyl-4H,6H-thieno[2,3-e][1,2,4]triazolo[3,4-c][1,4]oxazepin-2-yl)ethynyl)-1H-pyrazol-1-yl)-3-(2-hydroxyethyl)azetidine-1-carboxylate (28). Bis-(triphenylphosphine)palladium chloride (281 mg, 0.4 mmol, 0.1 equiv) and copper(I) iodide (152 mg, 0.8 mmol, 0.2 equiv) were added sequentially to a solution of compound **19** (1.51 g, 4.0 mmol, 1.0 equiv) in DMF (8.0 mL). The solution was degassed under sonication and refilled with argon three times. Then, a solution of compound **27** (1.40 g, 4.8 mmol, 1.2 equiv) in DMF (4.0 mL) was added and the solution was degassed another three times. Then, triethylamine (TEA, 8.0 mL) was added. The solution was degassed

another three times. The resulting solution was stirred at 80 °C for 5 h. After cooling to ambient temperature, the solution was diluted with EtOAc (100 mL) and saturated ammonium chloride (100 mL). The resulting solution was filtered through celite and washed with EtOAc (50 mL). The filtrate was poured into a separatory funnel. The collected organic layer was combined and dried over anhydrous sodium sulfate. After filtration, the solution was concentrated and the residue was purified by silica gel flash column chromatography eluting with hexane/EtOAc (10:1−1:100), then DCM/MeOH (100:1−10:1) to afford the title compound as a brown oil (2.16 g, 92% yield). UPLC-MS (ESI$^+$) calculated for $C_{31}H_{35}N_6O_4S$ [M + H]$^+$: 587.24, found 587.27.

Step d: 2-(3-(4-((3-Benzyl-9-methyl-4H,6H-thieno[2,3-e][1,2,4]-triazolo[3,4-c][1,4]oxazepin-2-yl)ethynyl)-1H-pyrazol-1-yl)azetidin-3-yl)ethan-1-ol (29). TFA (6.0 mL) was added at 0 °C to a solution of compound **28** (2.16 g, 3.68 mmol) in 24 mL of DCM. The resulting solution was stirred at ambient temperature for 2 h. The solvent was removed *in vacuo* as much as possible. The residue was diluted in MeCN (10 mL) and water (20 mL). Sodium carbonate (1.17 g, 11.04 mmol, 3.0 equiv) was added in small portions to this clear solution. The resulting solution was stirred at 60 °C for 2 h. UPLC-MS indicated that the trifluoroacetylated byproduct had been completely converted to the desired product. The solution was purified by preparative HPLC eluting with MeCN:water (0.1% TFA). Prior to concentration, an amount of N,N-diisopropylethylamine (DIPEA) equivalent to the residual TFA was added to afford the mixture of the desired product together with DIPEA/TFA salt as a white solid. UPLC-MS (ESI$^+$) calculated for $C_{26}H_{27}N_6O_2S$ [M + H]$^+$: 487.19, found 487.12.

Step e: 4-(3-(4-((3-Benzyl-9-methyl-4H,6H-thieno[2,3-e][1,2,4]-triazolo[3,4-c][1,4]oxazepin-2-yl)ethynyl)-1H-pyrazol-1-yl)-3-(2-hydroxyethyl)azetidin-1-yl)-2-(2,6-dioxopiperidin-3-yl)isoindoline-1,3-dione (30). DIPEA (0.96 mL, 5.52 mmol, 1.5 equiv) was added to a solution of the above HPLC-purified amine (**29**, 1.0 equiv) and 2-(2,6-dioxopiperidin-3-yl)-4-fluoroisoindoline-1,3-dione (1.12 g, 4.05 mmol, 1.1 equiv) in 10 mL of DMF. The resulting solution was stirred at 90 °C for 12 h. After cooling to ambient temperature, the solution was diluted with water (100 mL) and DCM (100 mL) and then transferred into a separatory funnel. After extraction twice, the organic layer was collected and dried over anhydrous sodium sulfate. After filtration, the residue was purified by silica gel flash column chromatography eluting with hexane/EtOAc (1:1−1:100), then DCM/MeOH (100:1−10:1) to afford the title compound as a yellow solid (2.02 g, 74% yield for two steps). UPLC-MS (ESI$^+$) calculated for $C_{39}H_{35}N_8O_6S$ [M + H]$^+$: 743.24, found 743.18.

Step f: 2-(3-(4-((3-Benzyl-9-methyl-4H,6H-thieno[2,3-e][1,2,4]-triazolo[3,4-c][1,4]oxazepin-2-yl)ethynyl)-1H-pyrazol-1-yl)-1-(2-(2,6-dioxopiperidin-3-yl)-1,3-dioxoisoindolin-4-yl)azetidin-3-yl)-acetaldehyde (31). Dess−Martin periodinane (2.31 g, 5.44 mmol, 2.0 equiv) was added to a solution of compound **30** (2.02 g, 2.72 mmol, 1.0 equiv) in 100 mL of DCM. Two drops of water were added, then the suspended solution was stirred vigorously at ambient temperature for 6 h when TLC indicated that most of starting material had been consumed. Then, DCM (100 mL) and water (100 mL) were added. The suspended solution was filtered through celite and washed with DCM (50 mL). The filtrate was transferred into a separatory funnel. After extraction, the organic layer was collected and dried over anhydrous sodium sulfate. After filtration and concentration, the residue was purified by silica gel flash column chromatography eluting with DCM/MeOH (100:1−10:1) to afford the title compound as a yellow solid (1.91 g, 95% yield). UPLC-MS (ESI$^+$) calculated for $C_{39}H_{33}N_8O_6S$ [M + H]$^+$: 741.22, found 741.15.

Step g: 4-(3-(4-((3-Benzyl-9-methyl-4H,6H-thieno[2,3-e][1,2,4]-triazolo[3,4-c][1,4]oxazepin-2-yl)ethynyl)-1H-pyrazol-1-yl)-3-(2-(4-methylpiperazin-1-yl)ethyl)azetidin-1-yl)-2-(2,6-dioxopiperidin-3-yl)isoindoline-1,3-dione (8, BD-9136). To a solution of compound **31** (938 mg, 1.26 mmol, 1.0 equiv) and 1-methylpiperazine (252 mg, 2.5 mmol, 2.0 equiv) in 25 mL of 1,2-dichloroethane was added sodium triacetoxyborohydride (401 mg, 1.89 mmol, 1.5 equiv). The solution was stirred at room temperature for 6 h. Another portion of sodium triacetoxyborohydride (401 mg) was added. The solution was

stirred at room temperature for another 6 h. The solution was transferred into a separatory funnel, and the solution was washed with saturated $NaHCO_3$ (aq). The combined organic layer was dried over anhydrous sodium sulfate. After filtration and concentration, the residue was purified by silica gel flash column chromatography eluting with ethyl acetate in hexane (10−100%), then methanol in dichloromethane (1−20%) to afford the title compound as yellow solid (863 mg, 83% yield). ^{1}H NMR (400 MHz, acetone-d_6) δ (ppm) 9.91 (s, 1H), 8.35 (s, 1H), 7.79 (s, 1H), 7.60 (dd, J = 8.4 Hz, J = 7.2 Hz, 1H), 7.33−7.27 (m, 4H), 7.24−7.17 (m, 2H), 6.87 (d, J = 8.4 Hz, 1H), 5.08 (dd, J = 12.8 Hz, J = 5.6 Hz, 1H), 4.81 (d, J = 9.6 Hz, 2H), 4.71 (s, 2H), 4.70 (s, 2H), 4.58 (d, J = 9.6 Hz, 2H), 4.12 (s, 2H), 3.00−2.89 (m, 1H), 2.81−2.71 (m, 2H), 2.68 (s, 3H), 2.60−2.40 (m, 10H), 2.29 (s, 3H), 2.21−2.14 (m, 3H); ^{13}C NMR (100 MHz, acetone-d_6) δ (ppm) 172.64, 170.13, 168.10, 167.71, 154.07, 151.26, 148.70, 142.99, 142.64, 139.40, 135.74, 134.85, 133.03, 131.37, 130.83, 129.57, 129.19, 127.43, 120.75, 117.21, 113.28, 112.82, 103.02, 89.71, 81.72, 68.43, 64.59, 63.03, 61.68, 55.50, 53.72, 53.41, 50.03, 45.73, 35.85, 34.42, 31.98, 23.38, 12.68; UPLC-MS (ESI$^+$) calculated for $C_{44}H_{45}N_{10}O_5S$ [M + H]$^+$: 825.33, found 825.31.

Antibodies and Reagents. Rabbit anti-BRD2 (Catalogue No. A302-583A), rabbit anti-BRD3 (Catalogue No. A302-368A-M), and rabbit anti-BRD4 (Catalogue No. A700-005) were purchased from Bethyl Laboratories, Inc., Montgomery, Texas. Mouse anti-GAPDH (Catalogue No. sc-47724) and all other antibodies were purchased from Santa Cruz Biotechnology, Inc., Dallas, TX.

Cell Lines. All of the cell lines were purchased from the ATCC and maintained in the medium following the datasheet from the ATCC. No more than 10 passages of cells from original stocks were used for this study.

Western Blot Analysis. Western blot analysis was performed as described previously.[23,25,26] The cells treated with indicated compounds were lysed in Radioimmunoprecipitation Assay Protein Lysis and Extraction Buffer (25 mmol/L Tris.HCl, pH 7.6, 150 mmol/L NaCl, 1% Nonidet P-40, 1% sodium deoxycholate, and 0.1% sodium dodecyl sulfate) containing proteinase inhibitor cocktail (Roche Diagnostics, Mannheim, Germany). Equal amounts of total proteins were electrophoresed through 10% sodium dodecyl sulfate (SDS)-polyacrylamide gels after the determination of protein concentration by bicinchoninic acid (BCA) assay (Fisher Scientific, Pittsburgh, PA). The separated protein bands were transferred onto PVDF membranes (GE Healthcare Life Sciences, Marlborough, MA) and blotted against different antibodies, as indicated. The blots were scanned, and the band intensities were quantified using GelQuant.-NET software provided by biochemlabsolutions.com. The relative mean intensity of target proteins was calculated after normalization to the intensity of glyceraldehyde-3-phosphate dehydrogenase bands from individual repeats.

Cell Growth Inhibition Assay. This assay was performed as described previously.[23,25,39] The cells were seeded at 1500/well in 96-well plates overnight. One day after the seeding, they were treated with indicated doses for each compound. The growth of the cells was evaluated by colorimetric WST-8 assay 4 days after the compound treatment following the instructions of the manufacturer, Cayman Chemical.

Bio-Layer Interferometry (BLI) Binding Assay. Purified recombinant BRD protein was first biotinylated using the Thermo EZ-Link long-chain biotinylation reagent. The BRD protein and biotinylation reagent were then mixed in a 1:1 molar ratio in phosphate-buffered saline (PBS) at 4 °C. This reaction mixture was incubated at 4 °C for 2 h. It was then dialyzed using Fisher Scientific 10K MWCO dialysis cassettes to remove unreacted biotinylation reagent. Then, the Bio-Layer Interferometry (BLI) binding assays were performed in 96-well microplates at rt with continuous 1000 RPM shaking using the Octet Red 96 system (ForteBio, Menlo Park, California). PBS with 0.1% bovine serum albumin (BSA), 0.01% Tween-20, and 2% DMSO was used as the assay buffer. Biotinylated BRD protein was tethered on Super Streptavidin (SSA) biosensors (ForteBio) by dipping sensors into 200 μL per well 10 μg/mL protein solutions. Average saturation response level of 8−10 nm was achieved

in 20 min. The measurement processes were all under computer control. Program procedures were established as follows: For the initial step, biosensors were washed in assay buffer for 60 s to form a baseline; the biosensors labeled with biotin-Menin were exposed to 100 nM compounds for the association and were monitored for 1200 s; then, the biosensors were moved back into assay buffer to disassociate for another 1800 s. Data were fit globally and generated automatically by Octet User software (version 9.0; Fortebio).

Proteomic Profiling. MV4;11 or MDA-MB-231 cells were treated with indicated compounds and concentrations for 3 h and then lysed in Radioimmunoprecipitation Assay Protein Lysis and Extraction Buffer (25 mmol/L Tris. HCl, pH 7.6, 150 mmol/L NaCl, 1% Nonidet P-40, 1% sodium deoxycholate, and 0.1% sodium dodecyl sulfate). Cell lysis samples (75 μg/condition) were then proteolyzed and labeled with TMT 10-plex by following the manufacturer's protocol (Thermo Fisher). Briefly, upon reduction and alkylation of cysteines, the proteins were precipitated by adding 6 volumes of ice-cold acetone followed by overnight incubation at −20 °C. The precipitate was spun down, and the pellet was allowed to air-dry. The pellet was resuspended in 0.1 M tetraethylammonium bromide and overnight digestion with trypsin (1:50; enzyme: protein) at 37 °C was performed with constant mixing using a thermomixer. The TMT 10-plex reagents were dissolved in 41 μL of anhydrous MeCN, and labeling was performed by transferring the entire digest to a TMT reagent vial and incubating at rt for 1 h. The reaction was quenched by adding 8 μL of 5% hydroxylamine and a further 15 min incubation. Labeled samples were mixed and dried using a Vacufuge. An offline fractionation of the combined sample (∼200 μg) into 10 fractions was performed using high-pH reversed-phase peptide fractionation kit according to the manufacturer's protocol (Pierce; Cat #84868). Fractions were dried and reconstituted in 12 μL of 0.1% formic acid/ 2% MeCN in preparation for liquid chromatography and tandem mass spectrometry (LC-MS/MS) analysis. The average difference from triplicates (fold change) between the compounds treated samples and vehicle-treated samples was plotted against the p-values calculated from the statistical analysis between the treatments.

Ternary Complex Formation Assays. The homogeneous time-resolved fluorescence (HTRF) assay was employed to assess the formation of ternary complex for a BRD degrader molecule with a recombinant individual bromodomain (BD1 or BD2) protein of BRD2, BRD3, or BRD4 and recombinant human cereblon. The HTRF assay was performed in OptiPlate-384 white plates (PerkinElmer, cat. No.: 6007290) with a total volume of 20 μL per well. 5 μL of His-BRD protein and 5 μL of Biotinylated-CRBN in the assay buffer (PBS pH = 7.4, 0.1% BSA) were added to the plate with the final assay concentration for both proteins to be 200 nM. 5 μL of a test compound at different concentrations was added to the plate, followed by addition of 5 μL of the mixture of HTRF Mab Anti-6His Tb Gold (PerkinElmer, cat. No. 61HI2TLB) and HTRF Streptavidin-XL665 (PrkinElmer, cat. No. 610saxlb). The plate was incubated at room temperature for 1 h in the dark with gentle shaking and was read by a microplate reader (CLARIOstar Plus, BMG LABTECH) for optimal signal detection at 620 and 665 nm. The ratio of 665/620 nm was used to measure the ternary complex formation.

***In Vivo* Pharmacodynamic and Efficacy Studies.** To develop MV4;11 or MDA-MB-231 xenografts, five million cells in 50% Matrigel were injected subcutaneously into SCID mice. For pharmacodynamics studies, when tumors reached 100−200 mm^3, mice were treated with vehicle control or the indicated dose of the drug, sacrificed at indicated time points, and tumor tissue was harvested for analyses.

For *in vivo* efficacy experiments, when tumors reached 80−200 mm^3, the mice were randomized into groups. Vehicle control (10% PEG400: 3% Cremophor: 87% PBS, or 2% TPGS:98% PEG200) was given at the dose and with the duration indicated. Tumor sizes and animal weights were measured 2−3 times per week. Tumor volume (mm^3) = (length × width^2)/2. Tumor growth inhibition was calculated as TGI (%) = $(V_c − V_t)/(V_c − V_o)$ × 100, where V_c and V_t are the median of control and treated groups at the end of the study and V_o at the start. All of the *in vivo* studies were performed

under an animal protocol (PRO00005315) approved by the University Committee on Use and Care of Animals of the University of Michigan, in accordance with the recommendations in the Guide for the Care and Use of Laboratory Animals of the National Institutes of Health.

Statistical Analysis. Statistical analysis was performed using analysis of variance, followed when appropriate, by post hoc testing with Scheffé's test.[39] For *in vivo* studies, the significance (*P*) was calculated by the Student *t*-test. *P* value < 0.05 was used as a criterion for statistical significance in comparisons between any two groups.

■ ASSOCIATED CONTENT

ⓈⒾ Supporting Information

The Supporting Information is available free of charge at https://pubs.acs.org/doi/10.1021/acs.jmedchem.3c00520.

Western blots of BRD2-4 proteins in the MV4;11 cell line treated with compounds **1**-**8**; kinetic binding sensorgrams of inhibitor QCA276 and representative degraders by bio-layer interferometry (BLI) assay; blocking experiment to determine the mechanism of action of BRD4 degradation by BD-7148 (**5**); Western blots of BRD2-4 proteins in 8 cancer cell lines treated with BD-7148 (**5**); quantification of western blots of BRD2-4 proteins in 8 cancer cell lines treated with BD-7148 (**5**); Western blots of BRD2-4 proteins in 8 cancer cell lines treated with BD-9136 (**8**); quantification of western blots of BRD2-4 proteins in 8 cancer cell lines treated with BD-9136 (**8**); cell growth inhibition curves of QCA276, BD-7148 and BD-9136 in 8 cancer cell lines; pharmacodynamic evaluation of QAC276 in MV4;11 and MDA-MB-231 xenograft tumors in mice; ^{1}H and ^{13}C NMR, UPLC-MS spectra of BD-9136 (HJ-9136); and UPLC-MS spectra for 6 other compounds (PDF)

A molecular string file for all of the final target compounds (CSV)

■ AUTHOR INFORMATION

Corresponding Author

Shaomeng Wang − *Department of Internal Medicine, University of Michigan, Ann Arbor, Michigan 48109, United States; Department of Pharmacology, Department of Medicinal Chemistry, and Rogel Cancer Center, University of Michigan, Ann Arbor, Michigan 48109, United States;* ⓞ orcid.org/0000-0002-8782-6950; Phone: 734-615-0362; Email: shaomeng@umich.edu; Fax: 734-647-9647

Authors

Jiantao Hu − *Department of Internal Medicine, University of Michigan, Ann Arbor, Michigan 48109, United States;* ⓞ orcid.org/0009-0007-4782-8779

Biao Hu − *Department of Internal Medicine, University of Michigan, Ann Arbor, Michigan 48109, United States;* ⓞ orcid.org/0000-0002-4691-6490

Fuming Xu − *Department of Internal Medicine, University of Michigan, Ann Arbor, Michigan 48109, United States*

Mi Wang − *Department of Internal Medicine, University of Michigan, Ann Arbor, Michigan 48109, United States*

Chong Qin − *Department of Internal Medicine, University of Michigan, Ann Arbor, Michigan 48109, United States;* ⓞ orcid.org/0000-0001-8108-1698

Donna McEachern − *Department of Internal Medicine, University of Michigan, Ann Arbor, Michigan 48109, United States*

Jeanne Stuckey − *Life Sciences Institute and Rogel Cancer Center, University of Michigan, Ann Arbor, Michigan 48109, United States*

Complete contact information is available at:
https://pubs.acs.org/10.1021/acs.jmedchem.3c00520

■ ACKNOWLEDGMENTS

■ ABBREVIATIONS USED

AML, acute myeloid leukemia; BET, bromodomain and extraterminal domain; BLI, Bio-Layer Interferometry; BRD4, bromodomain-containing protein 4; BRD2, bromodomain-containing protein 2; BRD3, bromodomain-containing protein 3; BD1, bromodomain 1; BD2, bromodomain 2; BPO, benzoyl peroxide; CDI, 1,1′-carbonyldiimidazole; CRBN, cereblon; DC_{50}, concentration needed to reduce protein by 50%; DMSO, dimethyl sulfoxide; DIPEA, *N,N*-diisopropylethylamine; DMA, *N,N*-dimethylacetamide; DMF, *N,N*-dimethylformamide; DMP, Dess−Martin periodinane; HATU, hexafluorophosphate azabenzotriazole tetramethyl uronium; HPLC, high-performance liquid chromatography; GAPDH, glyceraldehyde-3-phosphate dehydrogenase; NBS, *N*-bromosuccinimide; NIS, *N*-iodosuccinimide; NMR, nuclear magnetic resonance; PBS, phosphate-buffered saline; POI, protein of interest; PROTAC, proteolysis targeting chimera; PyBOP, benzotriazol-1-yl-oxytripyrrolidinophosphonium hexafluorophosphate; qPCR, quantitative polymerase chain reaction; TEA, trimethylamine; TBAF, tetra-*n*-butylammonium fluoride; THF, tetrahydrofuran; TFA, trifluoroacetic acid; VHL, von Hippel-Lindau

■ REFERENCES

(1) Belkina, A. C.; Denis, G. V. BET domain co-regulators in obesity, inflammation and cancer. *Nat. Rev. Cancer* 2012, 12, 465−77.

(2) Filippakopoulos, P.; Picaud, S.; Mangos, M.; Keates, T.; Lambert, J. P.; Barsyte-Lovejoy, D.; Felletar, I.; Volkmer, R.; Muller, S.; Pawson, T.; Gingras, A. C.; Arrowsmith, C. H.; Knapp, S. Histone recognition and large-scale structural analysis of the human bromodomain family. *Cell* 2012, 149, 214−31.

(3) Filippakopoulos, P.; Qi, J.; Picaud, S.; Shen, Y.; Smith, W. B.; Fedorov, O.; Morse, E. M.; Keates, T.; Hickman, T. T.; Felletar, I.; Philpott, M.; Munro, S.; McKeown, M. R.; Wang, Y. C.; Christie, A. L.; West, N.; Cameron, M. J.; Schwartz, B.; Heightman, T. D.; La Thangue, N.; French, C. A.; Wiest, O.; Kung, A. L.; Knapp, S.; Bradner, J. E. Selective inhibition of BET bromodomains. *Nature* 2010, 468, 1067−1073.

(4) Nicodeme, E.; Jeffrey, K. L.; Schaefer, U.; Beinke, S.; Dewell, S.; Chung, C. W.; Chandwani, R.; Marazzi, I.; Wilson, P.; Coste, H.; White, J.; Kirilovsky, J.; Rice, C. M.; Lora, J. M.; Prinjha, R. K.; Lee, K.; Tarakhovsky, A. Suppression of inflammation by a synthetic histone mimic. *Nature* 2010, 468, 1119−1123.

(5) Trojer, P. Targeting BET Bromodomains in Cancer. *Annu. Rev. Cancer Biol.* 2022, 6, 313−336.

(6) Sun, Y. L.; Han, J.; Wang, Z. Z.; Li, X. N.; Sun, Y. H.; Hu, Z. B. Safety and Efficacy of Bromodomain and Extra-Terminal Inhibitors for the Treatment of Hematological Malignances and Solid Tumors: A Systematic Study of Clinical Trials. *Front. Pharmacol.* 2021, 11, No. 621093.

(7) Doroshow, D. B.; Eder, J. P.; LoRusso, P. M. BET inhibitors: a novel epigenetic approach. *Ann. Oncol.* 2017, 28, 1776−1787.

(8) Tremblay, D.; Mesa, R. Novel treatments for myelofibrosis: beyond JAK inhibitors. *Int. J. Hematol.* 2022, 115, 645−658.

(9) Schwalm, M. P.; Knapp, S. BET bromodomain inhibitors. *Curr. Opin. Chem. Biol.* 2022, 68, No. 102148.

(10) Petretich, M.; Demont, E. H.; Grandi, P. Domain-selective targeting of BET proteins in cancer and immunological diseases. *Curr. Opin. Chem. Biol.* 2020, 57, 184−193.

(11) Gilan, O.; Rioja, I.; Knezevic, K.; Bell, M. J.; Yeung, M. M.; Harker, N. R.; Lam, E. Y. N.; Chung, C. W.; Bamborough, P.; Petretich, M.; Urh, M.; Atkinson, S. J.; Bassil, A. K.; Roberts, E. J.; Vassiliadis, D.; Burr, M. L.; Preston, A. G. S.; Wellaway, C.; Werner, T.; Gray, J. R.; Michon, A. M.; Gobbetti, T.; Kumar, V.; Soden, P. E.; Haynes, A.; Vappiani, J.; Tough, D. F.; Taylor, S.; Dawson, S. J.; Bantscheff, M.; Lindon, M.; Drewes, G.; Demont, E. H.; Daniels, D. L.; Grandi, P.; Prinjha, R. K.; Dawson, M. A. Selective targeting of BD1 and BD2 of the BET proteins in cancer and immunoinflammation. *Science* 2020, 368, 387−394.

(12) Faivre, E. J.; McDaniel, K. F.; Albert, D. H.; Mantena, S. R.; Plotnik, J. P.; Wilcox, D.; Zhang, L.; Bui, M. H.; Sheppard, G. S.; Wang, L.; Sehgal, V.; Lin, X.; Huang, X.; Lu, X.; Uziel, T.; Hessler, P.; Lam, L. T.; Bellin, R. J.; Mehta, G.; Fidanze, S.; Pratt, J. K.; Liu, D.; Hasvold, L. A.; Sun, C.; Panchal, S. C.; Nicolette, J. J.; Fossey, S. L.; Park, C. H.; Longenecker, K.; Bigelow, L.; Torrent, M.; Rosenberg, S. H.; Kati, W. M.; Shen, Y. Selective inhibition of the BD2 bromodomain of BET proteins in prostate cancer. *Nature* 2020, 578, 306−310.

(13) Liu, Z.; Chen, H.; Wang, P.; Li, Y.; Wold, E. A.; Leonard, P. G.; Joseph, S.; Brasier, A. R.; Tian, B.; Zhou, J. Discovery of Orally Bioavailable Chromone Derivatives as Potent and Selective BRD4 Inhibitors: Scaffold Hopping, Optimization, and Pharmacological Evaluation. *J. Med. Chem.* 2020, 63, 5242−5256.

(14) Divakaran, A.; Scholtz, C. R.; Zahid, H.; Lin, W.; Griffith, E. C.; Lee, R. E.; Chen, T.; Harki, D. A.; Pomerantz, W. C. K. Development of an N-Terminal BRD4 Bromodomain-Targeted Degrader. *ACS Med. Chem. Lett.* 2022, 13, 1621−1627.

(15) Sakamoto, K. M.; Kim, K. B.; Kumagai, A.; Mercurio, F.; Crews, C. M.; Deshaies, R. J. Protacs: chimeric molecules that target proteins to the Skp1-Cullin-F box complex for ubiquitination and degradation. *Proc. Natl. Acad. Sci. U.S.A.* 2001, 98, 8554−9.

(16) Winter, G. E.; Buckley, D. L.; Paulk, J.; Roberts, J. M.; Souza, A.; Dhe-Paganon, S.; Bradner, J. E. DRUG DEVELOPMENT. Phthalimide conjugation as a strategy for in vivo target protein degradation. *Science* 2015, 348, 1376−81.

(17) Bondeson, D. P.; Crews, C. M. Targeted Protein Degradation by Small Molecules. *Annu. Rev. Pharmacol. Toxicol.* 2017, 57, 107−123.

(18) Li, K.; Crews, C. M. PROTACs: past, present and future. *Chem. Soc. Rev.* 2022, 51, 5214−5236.

(19) Chirnomas, D.; Hornberger, K. R.; Crews, C. M. Protein degraders enter the clinic - a new approach to cancer therapy. *Nat. Rev. Clin. Oncol.* 2023, 20, 265−278.

(20) Zengerle, M.; Chan, K. H.; Ciulli, A. Selective Small Molecule Induced Degradation of the BET Bromodomain Protein BRD4. *ACS Chem. Biol.* 2015, 10, 1770−7.

(21) Lu, J.; Qian, Y.; Altieri, M.; Dong, H.; Wang, J.; Raina, K.; Hines, J.; Winkler, J. D.; Crew, A. P.; Coleman, K.; Crews, C. M. Hijacking the E3 Ubiquitin Ligase Cereblon to Efficiently Target BRD4. *Chem. Biol.* 2015, 22, 755−63.

(22) Raina, K.; Lu, J.; Qian, Y.; Altieri, M.; Gordon, D.; Rossi, A. M.; Wang, J.; Chen, X.; Dong, H.; Siu, K.; Winkler, J. D.; Crew, A. P.; Crews, C. M.; Coleman, K. G. PROTAC-induced BET protein degradation as a therapy for castration-resistant prostate cancer. *Proc. Natl. Acad. Sci. U.S.A.* 2016, 113, 7124−9.

(23) Bai, L.; Zhou, B.; Yang, C. Y.; Ji, J.; McEachern, D.; Przybranowski, S.; Jiang, H.; Hu, J.; Xu, F.; Zhao, Y.; Liu, L.; Fernandez-Salas, E.; Xu, J.; Dou, Y.; Wen, B.; Sun, D.; Meagher, J.; Stuckey, J.; Hayes, D. F.; Li, S.; Ellis, M. J.; Wang, S. Targeted Degradation of BET Proteins in Triple-Negative Breast Cancer. *Cancer Res.* 2017, 77, 2476−2487.

(24) Gadd, M. S.; Testa, A.; Lucas, X.; Chan, K. H.; Chen, W.; Lamont, D. J.; Zengerle, M.; Ciulli, A. Structural basis of PROTAC cooperative recognition for selective protein degradation. *Nat. Chem. Biol.* 2017, 13, 514−521.

(25) Qin, C.; Hu, Y.; Zhou, B.; Fernandez-Salas, E.; Yang, C. Y.; Liu, L.; McEachern, D.; Przybranowski, S.; Wang, M.; Stuckey, J.; Meagher, J.; Bai, L.; Chen, Z.; Lin, M.; Yang, J.; Ziazadeh, D. N.; Xu, F.; Hu, J.; Xiang, W.; Huang, L.; Li, S.; Wen, B.; Sun, D.; Wang, S. Discovery of QCA570 as an Exceptionally Potent and Efficacious Proteolysis Targeting Chimera (PROTAC) Degrader of the Bromodomain and Extra-Terminal (BET) Proteins Capable of Inducing Complete and Durable Tumor Regression. *J. Med. Chem.* 2018, 61, 6685−6704.

(26) Zhou, B.; Hu, J.; Xu, F.; Chen, Z.; Bai, L.; Fernandez-Salas, E.; Lin, M.; Liu, L.; Yang, C. Y.; Zhao, Y.; McEachern, D.; Przybranowski, S.; Wen, B.; Sun, D.; Wang, S. Discovery of a Small-Molecule Degrader of Bromodomain and Extra-Terminal (BET) Proteins with Picomolar Cellular Potencies and Capable of Achieving Tumor Regression. *J. Med. Chem.* 2018, 61, 462−481.

(27) Nowak, R. P.; DeAngelo, S. L.; Buckley, D.; He, Z.; Donovan, K. A.; An, J.; Safaee, N.; Jedrychowski, M. P.; Ponthier, C. M.; Ishoey, M.; Zhang, T.; Mancias, J. D.; Gray, N. S.; Bradner, J. E.; Fischer, E. S. Plasticity in binding confers selectivity in ligand-induced protein degradation. *Nat. Chem. Biol.* 2018, 14, 706−714.

(28) Yang, C. Y.; Qin, C.; Bai, L.; Wang, S. Small-molecule PROTAC degraders of the Bromodomain and Extra Terminal (BET) proteins - A review. *Drug Discovery Today Technol.* 2019, 31, 43−51.

(29) Blake, R. A.; Dragovich, P.; Gazzard, L. J.; Kaufman, S.; Kleinheinz, T.; Pillow, T.; Staben, S.; Wei, B. Tert-butyl (s)-2-(4-(phenyl)-6h-thieno[3,2-f][1,2,4]triazolo[4,3-a] [1,4]diazepin-6-yl) acetate derivatives and related compounds as bromodomain BRD4 inhibitors for treating cancer. WO2020/055976 A1.

(30) Shergalis, A. G.; Marin, V. L.; Rhee, D. Y.; Senaweera, S.; McCloud, R. L.; Ronau, J. A.; Hutchins, C. W.; McLoughlin, S.; Woller, K. R.; Warder, S. E.; Vasudevan, A.; Reitsma, J. M. CRISPR Screen Reveals BRD2/4 Molecular Glue-like Degrader via Recruitment of DCAF16. *ACS Chem. Biol.* 2023, 18, 331−339.

(31) Kaneshige, A.; Bai, L.; Wang, M.; McEachern, D.; Meagher, J. L.; Xu, R.; Wang, Y.; Jiang, W.; Metwally, H.; Kirchhoff, P. D.; Zhao,

L.; Jiang, H.; Wang, M.; Wen, B.; Sun, D.; Stuckey, J. A.; Wang, S., A selective small-molecule STAT5 PROTAC degrader capable of achieving tumor regression in vivo. *Nat. Chem. Biol.* **2023**, DOI: 10.1038/s41589-022-01248-4.

(32) Bai, L.; Zhou, H.; Xu, R.; Zhao, Y.; Chinnaswamy, K.; McEachern, D.; Chen, J.; Yang, C. Y.; Liu, Z.; Wang, M.; Liu, L.; Jiang, H.; Wen, B.; Kumar, P.; Meagher, J. L.; Sun, D.; Stuckey, J. A.; Wang, S. A Potent and Selective Small-Molecule Degrader of STAT3 Achieves Complete Tumor Regression In Vivo. *Cancer Cell* **2019**, *36*, 498−511e17.

(33) Zhou, H.; Bai, L.; Xu, R.; Zhao, Y.; Chen, J.; McEachern, D.; Chinnaswamy, K.; Wen, B.; Dai, L.; Kumar, P.; Yang, C. Y.; Liu, Z.; Wang, M.; Liu, L.; Meagher, J. L.; Yi, H.; Sun, D.; Stuckey, J. A.; Wang, S. Structure-Based Discovery of SD-36 as a Potent, Selective, and Efficacious PROTAC Degrader of STAT3 Protein. *J. Med. Chem.* **2019**, *62*, 11280−11300.

(34) Nalawansha, D. A.; Crews, C. M. PROTACs: An Emerging Therapeutic Modality in Precision Medicine. *Cell Chem. Biol.* **2020**, *27*, 998−1014.

(35) Kofink, C.; Trainor, N.; Mair, B.; Wohrle, S.; Wurm, M.; Mischerikow, N.; Roy, M. J.; Bader, G.; Greb, P.; Garavel, G.; Diers, E.; McLennan, R.; Whitworth, C.; Vetma, V.; Rumpel, K.; Scharnweber, M.; Fuchs, J. E.; Gerstberger, T.; Cui, Y.; Gremel, G.; Chetta, P.; Hopf, S.; Budano, N.; Rinnenthal, J.; Gmaschitz, G.; Mayer, M.; Koegl, M.; Ciulli, A.; Weinstabl, H.; Farnaby, W. A selective and orally bioavailable VHL-recruiting PROTAC achieves SMARCA2 degradation in vivo. *Nat. Commun.* **2022**, *13*, No. 5969.

(36) Cantley, J.; Ye, X.; Rousseau, E.; Januario, T.; Hamman, B. D.; Rose, C. M.; Cheung, T. K.; Hinkle, T.; Soto, L.; Quinn, C.; Harbin, A.; Bortolon, E.; Chen, X.; Haskell, R.; Lin, E.; Yu, S. F.; Del Rosario, G.; Chan, E.; Dunlap, D.; Koeppen, H.; Martin, S.; Merchant, M.; Grimmer, M.; Broccatelli, F.; Wang, J.; Pizzano, J.; Dragovich, P. S.; Berlin, M.; Yauch, R. L. Selective PROTAC-mediated degradation of SMARCA2 is efficacious in SMARCA4 mutant cancers. *Nat. Commun.* **2022**, *13*, No. 6814.

(37) Kaneshige, A.; Bai, L.; Wang, M.; McEachern, D.; Meagher, J. L.; Xu, R.; Kirchhoff, P. D.; Wen, B.; Sun, D.; Stuckey, J. A.; Wang, S. Discovery of a Potent and Selective STAT5 PROTAC Degrader with Strong Antitumor Activity In Vivo in Acute Myeloid Leukemia. *J. Med. Chem.* **2023**, *66*, 2717−2743.

(38) Cheung, K. L.; Kim, C.; Zhou, M. M. The Functions of BET Proteins in Gene Transcription of Biology and Diseases. *Front. Mol. Biosci.* **2021**, *8*, No. 728777.

(39) Hu, J.; Hu, B.; Wang, M.; Xu, F.; Miao, B.; Yang, C. Y.; Wang, M.; Liu, Z.; Hayes, D. F.; Chinnaswamy, K.; Delproposto, J.; Stuckey, J.; Wang, S. Discovery of ERD-308 as a Highly Potent Proteolysis Targeting Chimera (PROTAC) Degrader of Estrogen Receptor (ER). *J. Med. Chem.* **2019**, *62*, 1420−1442.